Fermilab Library
0 1160 0025844 9
INLO-PUB-J.93

INLO-PUB-8/93

Higher order QCD corrections to deep inelastic scattering*

W.L. van Neerven

Instituut-Lorentz
University of Leiden
P.O. Box 9506
2300 RA Leiden
The Netherlands

FERMILAB
JUL 16 1993
LIBRARY

Abstract

We discuss the calculation of the order α_s^2 QCD contributions to the deep inelastic coefficient functions for polarized and unpolarized deep inelastic lepton–hadron scattering. These corrections receive some contributions from production mechanisms which do not appear up to the order α_s level. The effect of these higher order corrections on the polarized and unpolarized structure functions will be analyzed. The calculations reveal large corrections in the small x–region accessible at HERA as well as in the large x–region explored by fixed target experiments.

*Lectures given at the XXI International Meeting on Fundamental Physics, Mira Flores de la Sierra, Madrid, May 9–15th, 1993

1 Introduction

Deep inelastic lepton–hadron scattering experiments, started by the SLAC-MIT group [1] at the end of the sixties, opened a new era in the study of strong interaction physics. These experiments revealed that hadrons are composed of pointlike constituents, called partons, which were later on identified as quarks and gluons. In the framework of the parton model [2] the early data could be interpreted by assuming that the scattering process between the lepton and the partons is incoherent. In this way one could explain the apparent scaling behaviour of the hadronic structure functions appearing in the deep inelastic lepton–hadron cross sections. In addition one could derive various sum rules which can be expressed as integrals over the structure functions and their validity was confirmed by the early data. Considerable progress was made after the advent of Quantum Chromo Dynamics (QCD) [3], a non–abelian (here SU(3)) gauge field theory, which describes the strong interaction between the quarks and gluons inside the hadron. In particular it is supposed to give an explanation for the phenomenon that the quarks and gluons are confined [4] in all existing hadrons. Another important feature of QCD is asymptotic freedom [5] which implies that the renormalization group improved (running) coupling constant $\alpha_s(R^2)$ goes to zero when the renormalization scale R tends to infinity. This property allows us to make an expansion in α_s of the perturbative part of the hadronic structure functions which are represented by the Altarelli-Parisi (AP) splitting functions [6] and the coefficient functions. If these corrections are resummed via the renormalization group (or Altarelli-Parisi) equations one can explain the scale dependence of the hadronic structure functions which was confirmed by the second generation of deep inelastic lepton hadron experiments [7]. For the most recent experiments see [8]–[12]. Until the middle of 1992 the AP splitting functions were calculated up to $\mathcal{O}(\alpha_s^2)$ [13]–[17] whereas the deep inelastic coefficient functions (also called Wilson coefficients) were known up to $\mathcal{O}(\alpha_s)$ only [18]–[20]. With the advent of HERA (DESY, Hamburg) [21] and the planned electron-proton facility at LEP $*$ LHC (CERN, Geneva) [22] a new generation of experiments will start to test QCD in kinematical regions which were inaccessible so far. We also would like to mention the experiments which will measure the spin structure functions of the proton with a higher accuracy than has been done until now. They will be carried out e.g. by SMC (CERN, Geneva) [23] and HERMES (DESY, Hamburg) [24]. Due to improved detection techniques and higher statistics of the data we expect that higher order QCD corrections beyond the next to leading order will become noticeable and therefore have to be calculated. This requires the calculation of the $\mathcal{O}(\alpha_s^3)$ contributions to the AP splitting functions and the $\mathcal{O}(\alpha_s^2)$ contributions to the coefficient functions in particular for unpolarized lepton hadron scattering. Recently the calculation of the $\mathcal{O}(\alpha_s^2)$ contributions to the unpolarized and polarized coefficient functions have been finished by us, see [25]–[29], and the results will be discussed in these lectures. The lectures will be organized as follows. In section 2 we present the kinematics of deep inelastic lepton hadron scattering. In section 3 we show how the $\mathcal{O}(\alpha_s^2)$ contributions to the coefficient functions are calculated without going into explicit details. Here it will turn out that the procedure of mass factorization becomes much more complicated than in the case of the lowest order

corrections. In section 4 we discuss the properties of the coefficient functions where the latter show some large corrections in the small as well as in the large x-region. These corrections did not show up on the $\mathcal{O}(\alpha_s)$ level. In section 5 we show how the next to leading log description of the structure functions is modified by including the (α_s^2) contribution to the coefficient functions. The effect of the still missing $\mathcal{O}(\alpha_s^3)$ contributions to the AP splitting functions will be estimated.

2 Kinematics of deep inelastic lepton-hadron scattering

Deep inelastic lepton-hadron scattering is given by the reaction (see fig.1)

$$\ell_1(k_1) + H(p) \to \ell_2(k_2) + \text{“}X\text{”} \quad , \tag{2.1}$$

where ℓ_1, ℓ_2 denote the in- and outgoing leptons respectively and H stands for the hadron (mostly proton or neutron). The symbol "X" denotes any inclusive hadronic final state allowed by quantum number conservation laws. In lowest order of the electroweak coupling constant the reaction proceeds via the exchange of one of the intermediate vector bosons of the standard model, i.e., $V = \gamma, Z, W$ (see fig.1). Since the above process is inclusive with respect to the outgoing hadrons denoted by "X", only the outgoing lepton is detected. In these lectures we will discuss the neutral current reaction with $\ell_1 = \ell_2 = e, V = \gamma$ and the charged current reaction $\ell_1 = \nu_\mu(\bar{\nu}_\mu)$, $\ell_2 = \mu^-(\mu^+)$, $V = W^+(W^-)$. At large momentum transfer the neutral current interaction gets also contributions from Z-boson exchange. In this case the deep inelastic cross section becomes more complicated (for details see [21]). We will now treat the neutral current interaction with $V = \gamma$ (pure electromagnetism) in a little bit more detailed way. In the one photon exchange approximation (fig.1) the scattering amplitude is given by

$$T = ie^2 \frac{1}{q^2 + i\varepsilon} < k_2, \sigma_2 | j_\mu(0) | k_1, \sigma_1 >< P_n, \xi | J^\mu(0) | p, s > \quad . \tag{2.2}$$

Here $\sigma_1(\sigma_2)$ and s denote the spins of the in (out) going electron and proton respectively. The momentum and the quantum numbers (internal, external) of the hadronic state X are given by P_n and ξ. The electromagnetic current for the lepton and the hadron are given by j_μ and J^μ respectively. The differential cross section is given by

$$\begin{aligned} d\sigma \;=\; & \frac{1}{|\vec{v}_1 - \vec{v}_p|} \; \frac{1}{4E_1E_p} \; \frac{d^3\vec{k}_2}{(2\pi)^3\, 2E_2} \; \sum_{n,\xi} \; \frac{d^3\vec{P}_n}{(2\pi)^3\, 2E_n} \; |T|^2 \; \cdot \\ & (2\pi)^4\, \delta^{(4)}(k_1 + p - k_2 - P_n) \quad . \end{aligned} \tag{2.3}$$

Summation over the spins of the outgoing electron yields

$$|T|^2 = \frac{e^4}{q^4} L_{\mu\nu} \; < p, s | J^\mu(0) | P_n, \xi >< P_n, \xi | J^\nu(0) | p, s > \quad , \tag{2.4}$$

where the leptonic tensor is given by

$$\begin{aligned} L_{\mu\nu}(k_1,q,\sigma_1) &= \frac{1}{2}Tr(\not{k}_2+m)\gamma_\mu(\not{k}_1+m)(1+\gamma_5\not{\phi}_1)\gamma_\nu \\ &= 2\left[2k_{1\mu}k_{1\nu}-q_\mu k_{1\nu}-q_\nu k_{1\mu}+\frac{1}{2}g_{\mu\nu}q^2+2\,i\,m\,\varepsilon_{\mu\nu\alpha\beta}\,q^\alpha\sigma_1^\beta\right] \\ &= L^{[S]}_{\mu\nu}(k_1,q)+i\,L^{[A]}_{\mu\nu}\,(k_1,q,\sigma_1) \quad , \end{aligned} \tag{2.5}$$

where q denotes the momentum transfer $q = k_1 - k_2$. The leptonic tensor is split into a symmetric and antisymmetric part. The latter is due to the polarization σ_1 of the incoming electron. The hadronic tensor is defined by

$$W^{\mu\nu}(p,q,s) = \frac{1}{4\pi M}\int d^4z\, e^{iqz} < p,s|\,[J^\mu(z),J^\nu(0)]\,|p,s> \quad . \tag{2.6}$$

The above expression can be rewritten by inserting a complete set of intermediate states. Using the completeness relation one gets

$$1 = \sum_n |n><n| = \sum_{n,\xi}\frac{d^3P_n}{(2\pi)^3 2E_n}\,|P_n,\xi><P_n,\xi| \quad . \tag{2.7}$$

Inserting the above expression into (2.6) we obtain:

$$\begin{aligned} W^{\mu\nu}(p,q,s) &= \frac{1}{4\pi M}\sum_{n,\xi}\frac{d^3P_n}{(2\pi)^3\,2E_n}\int d^4z\,e^{iqz} \\ &\quad \{<p,s|J^\mu(z)|P_n,\xi><P_n,\xi|J^\nu(0)|p,s> \\ &\quad -<p,s|J^\nu(0)|P_n,\xi><P_n,\xi|J^\mu(z)|p,s>\} \quad . \end{aligned} \tag{2.8}$$

Using translation invariance

$$e^{iPz}J^\mu(0)\,e^{-iPz} = J^\mu(z) \quad , \tag{2.9}$$

where P is the four momentum operator with the properties

$$P_\mu|p,s>= p_\mu|p,s> \rightarrow \; e^{iPz}|p,s>= e^{ipz}|p,s> \quad , \tag{2.10}$$

equation (2.8) becomes

$$\begin{aligned} W^{\mu\nu}(p,q,s) &= \frac{1}{4\pi M}\sum_{n,\xi}\frac{d^3P_n}{(2\pi)^3\,2E_n} \\ &\quad \Big\{\delta^{(4)}(p+q-P_n)<p,s|J^\mu(0)|P_n,\xi><P_n,\xi|J^\nu(0)|p,s> \\ &\quad -\delta^{(4)}(q-p+P_n)<p,s|J^\nu(0)|P_n,\xi><P_n,\xi|J^\mu(0)|p,s>\Big\} \quad . \end{aligned} \tag{2.11}$$

The second delta function vanishes because its argument is always larger than zero. This can be shown as follows. In the rest frame of the proton we have: $p_0 = E_p = M, q_0 = E_1 - E_2 > 0$ and $P_{n,0} \geq M$. Therefore the delta-function has to vanish

in any frame because of Lorentz covariance. The property that $W^{\mu\nu}$ can be written as the Fourier transform of the expectation value of the commutator of two local currents is very important. Since the commutator vanishes for spacelike distances, i.e., $z^2 < 0$ one can prove that in the limit $-q^2, pq \to \infty$ the integral in (2.6) is dominated by the light cone behaviour of the current commutator (i.e. the behaviour near $z^2 = 0$). This allows us to make a light cone expansion of the two local currents. This property is characteristic for deep inelastic lepton hadron scattering and it does not appear when one studies other deep inelastic processes like massive lepton pair production (Drell-Yan process), heavy flavour production, direct photon production etc. If we calculate the differential cross section (2.3) in the rest frame of the proton the momenta are parametrized as follows

$$p = (M, 0) \ , \quad k_1 = E_1(1,0,0,1) \ , \quad k_2 = E_2(1,0,\sin\theta,\cos\theta) \ , \tag{2.12}$$

and the cross section reads (solid angle: $d\Omega_2 = \sin\theta\, d\theta\, d\phi$)

$$\frac{d^2\sigma}{dE_2 d\Omega_2} = \frac{\alpha^2}{q^4}\frac{E_2}{E_1} L_{\mu\nu}(k_1, q, \sigma_1) W^{\mu\nu}(p, q, s) \ . \tag{2.13}$$

Because of Lorentz covariance, conservation of the electromagnetic current J^μ and PT invariance (P = parity, T = time reversal) the hadronic tensor can be written as

$$\begin{aligned} W^{\mu\nu} &= \left(-g^{\mu\nu} + \frac{q^\mu q^\nu}{q^2}\right) W_1(pq, q^2) + \left(p^\mu - \frac{pq}{q^2}q^\mu\right)\left(p^\nu - \frac{pq}{q^2}q^\nu\right)\frac{W_2(pq,q^2)}{M^2} \\ &+ i\left[M\epsilon^{\mu\nu\lambda\tau} q_\lambda s_\tau G_1(pq, q^2) + \frac{1}{M}\epsilon^{\mu\nu\lambda\tau} q_\lambda (pq\, s_\tau - qs p_\tau)\, G_2(pq, q^2)\right] \\ &= W^{\mu\nu}_{[S]}(p,q) + i W^{\mu\nu}_{[A]}(p,q,s) \ , \end{aligned} \tag{2.14}$$

with $s \cdot p = 0$. Here W_i denotes the (proton) spin averaged structure functions and G_1 (longitudinal) and G_2 (transverse) stand for the spin structure functions of the proton respectively. There exists a third structure function called the longitudinal structure function $W_L(pq, q^2)$ which depends on W_1 and W_2. It is defined by

$$W_L(pq, q^2) = -W_1(pq, q^2) - \frac{(pq)^2}{M^2 q^2} W_2(pq, q^2) \ . \tag{2.15}$$

Using (2.5) and (2.14) the cross section in (2.13) can be written as

$$\frac{d^2\sigma}{dE_2 d\Omega_2} = \frac{\alpha^2}{q^4}\frac{E_2}{E_1}\left[L^{[S]}_{\mu\nu} W^{\mu\nu}_{[S]} - L^{[A]}_{\mu\nu} W^{\mu\nu}_{[A]}\right] \ . \tag{2.16}$$

The unpolarized cross section is obtained by averaging over the initial spin of the proton

$$\left(\frac{d^2\sigma}{dE_2 d\Omega_2}\right)_{unpol} = \frac{\alpha^2}{q^4}\frac{E_2}{E_1} L^{[S]}_{\mu\nu} W^{\mu\nu}_{[S]} \ . \tag{2.17}$$

The contraction of the two tensors is straightforward. Using the momentum assignment (2.12) in the rest frame of the proton we obtain

$$\left(\frac{d^2\sigma}{dE_2 d\Omega_2}\right)_{unpol} = \frac{\alpha^2}{4E_1^2 \sin^4\frac{\theta}{2}}\left[W_2(pq, q^2)\cos^2\frac{\theta}{2} + 2W_1(pq, q^2)\sin^2\frac{\theta}{2}\right] \ , \tag{2.18}$$

where we have neglected the mass of the proton M. The polarized cross section is derived from the asymmetry dA given by

$$dA = d\sigma(s,\sigma_1) - d\sigma(-s,\sigma_1) \quad . \tag{2.19}$$

Since the symmetric parts cancel in dA we find

$$\frac{d^2\sigma(s,\sigma_1)}{dE_2 d\Omega_2} - \frac{d^2\sigma(-s,\sigma_1)}{dE_2 d\Omega_2} = 2\frac{\alpha^2}{q^4}\frac{E_2}{E_1} L^{[A]}_{\mu\nu} W^{\mu\nu}_{[A]} \quad . \tag{2.20}$$

Any proton spin component normal to the scattering plane (here y-z plane) gives no effect (assuming T–invariance). It is therefore sufficient to give the two independent spin configurations for the proton spin parallel and transverse to the beam direction in the electron scattering plane. Here the incoming electrons are longitudinally polarized so that the polarization effects are not proportional to the lepton mass m. Specifically we choose

$$\sigma_1 = \frac{E_1}{m}(1,0,0,1) \stackrel{def}{=} \rightarrow \tag{2.21}$$

$$s_{\text{long}} = (0,0,0,1) \stackrel{\text{def}}{=} \rightarrow \tag{2.22}$$

$$s_{\text{trans}} = (0,0,1,0) \stackrel{\text{def}}{=} \uparrow \tag{2.23}$$

In the case the proton is longitudinally polarized we obtain

$$\frac{d^2\sigma^{\rightrightarrows}}{dE_2\, d\Omega_2} - \frac{d^2\sigma^{\rightleftarrows}}{dE_2\, d\Omega_2} = \frac{4\alpha^2}{q^2}\frac{E_2}{E_1}\Big[(E_1 + E_2\cos\theta)MG_1(pq,q^2) + q^2 G_2(pq,q^2)\Big] \quad , \tag{2.24}$$

where the upper (lower) arrow represents the electron (proton) spin. When the proton is transversely polarized we get

$$\frac{d^2\sigma^{\rightarrow\uparrow}}{dE_2 d\Omega_2} - \frac{d^2\sigma^{\rightarrow\downarrow}}{dE_2 d\Omega_2} = \frac{4\alpha^2}{q^2}\frac{E_2^2}{E_1}\sin\theta\left[MG_1(pq,q^2) + q^2 G_2(pq,q^2)\right] \quad . \tag{2.25}$$

where the left (rigth) arrow represents the electron (proton) spin.

The calculation of the cross section for the charged current reaction proceeds in the same way. In the one W-exchange approximation the scattering amplitude becomes

$$T = \frac{i}{\sqrt{2}} G_F \frac{M_W^2}{q^2 - M_W^2 + ie} < k_2,\sigma_2|j_\mu^{(\alpha)}(0)|k_1,\sigma_1 >< P_n,\xi|J^\mu_{(\alpha)}(0)|p,s > \quad , \tag{2.26}$$

where $\alpha = +$ refers to the reaction with a neutrino in the initial state which is mediated by W^+ exchange and $\alpha = -$ refers to the reaction with an anti–neutrino in the initial state which is mediated by W^- exchange. Notice that the charged current $J^\mu_{(\alpha)}$ changes the flavour of the state on which it works. For $\alpha = + : Q_{P_n} - Q_p = 1$ and for $\alpha = - : Q_{P_n} - Q_p = -1$ where Q_p denotes the charge of the state with

momentum p. In the rest frame of the hadron with momentum p the unpolarized cross section is given by

$$\frac{d^2\sigma}{dE_2 d\Omega_2} = \frac{1}{8}\frac{G_F^2}{(2\pi)^2}\left(\frac{M_W^2}{q^2 - M_W^2}\right)^2 \frac{E_2}{E_1} L^{(\alpha)}_{\mu\nu}(k_1, q)\, W^{\mu\nu}_{(\alpha)}(p, q) \tag{2.27}$$

Here G_F denotes the Fermi constant and the leptonic tensor is given by

$$L^{(\alpha)}_{\mu\nu} = 8\left[2k_{1\mu}k_{1\nu} - q_\nu k_{1\mu} - q_\mu k_{1\nu} + \frac{1}{2}g_{\mu\nu}q^2 + i\alpha\,\varepsilon_{\mu\nu\lambda\sigma}q^\lambda k_1^\sigma\right] \tag{2.28}$$

where we have neglected the lepton masses.
From Lorentz covariance it follows that the hadronic tensor can be written as

$$\begin{aligned} W^{\mu\nu}_{(\alpha)}(p,q) \;=\; & -\left(g^{\mu\nu} - \frac{q^\mu q^\nu}{q^2}\right) W_1^{(\alpha)}(pq, q^2) \\ & + \left(p^\mu - \frac{pq}{q^2}q^\mu\right)\left(p^\nu - \frac{pq}{q^2}q^\nu\right)\frac{W_2^{(\alpha)}(pq,q^2)}{M^2} \\ & -i\varepsilon^{\mu\nu\alpha\beta}p_\alpha q_\beta \frac{W_3^{(\alpha)}(pq,q^2)}{2M^2} + q^\mu q^\nu \frac{W_4^{(\alpha)}(pq,q^2)}{M^2} \\ & +(p^\mu q^\nu + p^\nu q^\mu)\frac{W_5^{(\alpha)}(pq,q^2)}{M^2} \\ & +i\,(p^\mu q^\nu - p^\nu q^\mu)\frac{W_6^{(\alpha)}(pq,q^2)}{M^2} \end{aligned} \tag{2.29}$$

Besides CP-invariance which leads to the vanishing of W_6 there are no other restrictions on $W^{\mu\nu}$. Notice that instead of W_1 we could also use the longitudinal structure function W_L defined in (2.15). Using (2.28) and (2.29) the cross section in (2.27) becomes

$$\begin{aligned} \frac{d^2\sigma^{(\alpha)}}{dE_2 d\Omega_2} \;=\; & \frac{G_F^2}{2\pi^2}E_2^2\left(\frac{M_W^2}{M_W^2 - q^2}\right)^2 \Big[2W_1^{(\alpha)}(pq,q^2)\sin^2\frac{\theta}{2} \\ & +W_2^{(\alpha)}(pq,q^2)\cos^2\frac{\theta}{2} \\ & -\alpha\, W_3^{(\alpha)}(pq,q^2)\frac{E_1+E_2}{M}\sin^2\frac{\theta}{2}\Big] \quad . \end{aligned} \tag{2.30}$$

Since we have neglected the lepton masses, the structure functions W_4 and W_5 drop out in the above cross section. Moreover in the leading twist approximation, where the weak current is conserved, they will vanish. Like in the electromagnetic case the hadronic structure tensor can be written as

$$W^{\mu\nu}_{(\alpha)}(p,q) = \frac{1}{4\pi M}\int d^4z\, e^{iqz} < p,s|\left[J^\mu_{(-\alpha)}(z)\,,\, J^\nu_{(\alpha)}(0)\right]|p,s> \tag{2.31}$$

The weak current is of the V-A type, i.e.,

$$J^\mu_{(\alpha)}(z) = V^\mu_{(\alpha)}(z) - A^\mu_{(\alpha)}(z) \tag{2.32}$$

where $V^{\mu}_{(\alpha)}$ and $A^{\mu}_{(\alpha)}(z)$ stand for the vector and axial vector respectively. Under charge conjugation they transform in the following way

$$C\,V^{\mu}_{(\alpha)}(z)\,C^{\dagger} = -V^{\mu}_{(-\alpha)}(z)^{\dagger} = -V^{\mu}_{(\alpha)}(z) \tag{2.33}$$

$$C\,A_{(\alpha)}(z)\,C^{\dagger} = A^{\mu}_{(-\alpha)}(z)^{\dagger} = A_{(\alpha)}(z) \tag{2.34}$$

The charge conjugation operator is denoted by C with $CC^{\dagger} = 1$. Since the strong interactions are invariant under charge conjugation hadrons and anti–hadrons are related i.e.

$$C|H;p,s> = |\bar{H};p,s> \quad , \tag{2.35}$$

where H and $\bar{H}$ denote the hadron and anti-hadron respectively. Using this property, one can derive a relation between the structure functions of hadrons and anti-hadrons. From the matrix element in (2.31) we can infer the following relation

$$\begin{aligned}
&< H;p,s|\left\{\left[V^{\mu}_{(-\alpha)}(z),V^{\nu}_{(\alpha)}(0)\right]+\left[A^{\mu}_{(-\alpha)}(z),A^{\mu}_{(\alpha)}(0)\right]\right\} \\
&-\left\{\left[A^{\mu}_{(-\alpha)}(z),V^{\nu}_{\alpha}(0)\right]+\left[V^{\mu}_{(-\alpha)}(z),A^{\nu}_{(\alpha)}(0)\right]\right\}|H;p,s> \\
&=< H;p,s|C^{\dagger}C\left(\left\{\left[V^{\mu}_{(-\alpha)}(z),V^{\nu}_{(\alpha)}(0)\right]+\left[A^{\mu}_{(-\alpha)}(z),A^{\nu}_{(\alpha)}(0)\right]\right\}\right. \\
&\left.-\left\{\left[A^{\mu}_{(-\alpha)}(z),V^{\nu}_{(\alpha)}(0)\right]+\left[V^{\mu}_{(-\alpha)}(z),A^{\nu}_{(\alpha)}(0)\right]\right\}\right)C^{\dagger}C|H;p,s> \\
&=< \bar{H};p,s|\left\{\left[CV^{\mu}_{(-\alpha)}(z)C^{\dagger},CV^{\nu}_{(\alpha)}(0)C^{\dagger}\right]+\left[CA^{\mu}_{(-\alpha)}(z)C^{\dagger},CA^{\nu}_{(\alpha)}(0)C^{\dagger}\right]\right\} \\
&-\left\{\left[CA^{\mu}_{(-\alpha)}(z)C^{\dagger},CV_{(\alpha)}(0)C^{\dagger}\right]+\left[CV^{\mu}_{(-\alpha)}(z)C^{\dagger},CA^{\nu}_{(\alpha)}C^{\dagger}\right]\right\}|\bar{H},p,s> \quad .
\end{aligned} \tag{2.36}$$

Using the charge conjugation relations in (2.33) and (2.34) the last expression in (2.36) can be written as

$$< \bar{H};p,s|\left\{\left[V^{\mu}_{(-\alpha)}(z),V^{\nu}_{(\alpha)}(0)\right]+\left[A^{\mu}_{(-\alpha)}(z),A^{\nu}_{(\alpha)}(0)\right]\right\} \tag{2.37}$$

$$+\left\{\left[A^{\mu}_{(-\alpha)}(z),V_{(\alpha)}(0)\right]\left[V^{\mu}_{(-\alpha)}(z),A^{\nu}_{(\alpha)}(0)\right]\right\}\ |\bar{H};\,p,s> \quad . \tag{2.38}$$

The commutators $[V,V]$ and $[A,A]$ contribute to the structure functions $W_k(k=1,2)$ and the commutators $[A,V]$ and $[V,A]$ contribute to W_3. Hence we have the relations

$$W^{(\alpha)}_{k,H}(pq,q^2) = W^{(\alpha)}_{k,\bar{H}}(pq,q^2) \quad . \qquad k=1,2 \quad , \tag{2.39}$$

$$W^{(\alpha)}_{3,H}(pq,q^2) = -W^{(\alpha)}_{3,\bar{H}}(pq,q^2) \quad . \tag{2.40}$$

In case the hadron is a charge conjugate eigenstate like e.g. the pion $W^{(\alpha)}_3 = 0$. Furthermore we can also derive that all QCD corrections to $W^{(\alpha)}_3$ which originate from parton subprocesses, where the parton in the initial state is an eigenstate of

charge conjugation like the photon, also vanish. Since $W_k^{(\alpha)}$ does not depend on the colour index the above statement also holds for the gluon.

One can derive many more relations between the deep inelastic structure functions (for details, see [2]). In the literature one very often redefines the structure functions in order to make them dimensionless. Introducing the Bjorken scaling variable $x = Q^2/2pq$ with $q^2 = -Q^2 < 0$ one defines

$$MW_1(pq, q^2) = F_1(x, Q^2) \quad , \tag{2.41}$$

$$\frac{pq}{M}\, W_2(pq, q^2) = F_k(x, Q^2) \quad , \qquad k = 2, 3 \quad , \tag{2.42}$$

$$\frac{MQ^2}{pq}\, W_L(pq, q^2) = F_L(x, Q^2) \quad , \tag{2.43}$$

$$M\, pq\, G_1(pq, q^2) = g_1(x, Q^2) \quad , \tag{2.44}$$

$$\frac{(pq)^2}{M}\, G_2(pq, q^2) = g_2(x, Q^2) \quad . \tag{2.45}$$

Also the deep inelastic cross sections are very often presented in a different way. Here we introduce a second scaling variable y with $y = pq/pk_1$. In the rest frame of the hadron we have

$$E_2 = E_1(1-y) \ , \quad \sin^2\frac{\theta}{2} = \frac{M^2x^2y^2}{Q^2(1-y)} \ , \quad \cos^2\frac{\theta}{2} = 1 - \frac{Mxy}{2(1-y)E_1} \quad . \tag{2.46}$$

The deep inelastic cross sections can then be rewritten in the following form. In the case of the pure electromagnetic process the unpolarized cross section (2.18) becomes

$$\left(\frac{d^2\sigma}{dxdy}\right)_{\text{unpol}} = \frac{4\pi\alpha^2}{(Q^2)^2}(S - M^2)\left[\left\{1 - y - \frac{M^2xy}{S - M^2}\right\} F_2(x, Q^2) + xy^2 F_1(x, Q^2)\right] \quad , \tag{2.47}$$

where S is the CM energy of the lepton hadron system (here $S = 2ME_1 + M^2$). The polarized cross sections (2.24) and (2.25) are equal to

$$\frac{d^2\sigma^{\rightrightarrows}}{dxdy} - \frac{d^2\sigma^{\rightleftarrows}}{dxdy} = \frac{8\pi\alpha^2}{q^2}\left[\left(2 - y - \frac{2M^2xy}{S - M^2}\right) g_1(x, Q^2) - \frac{4M^2x}{S - M^2} g_2(x, Q^2)\right] \tag{2.48}$$

$$\frac{d^2\sigma^{\rightarrow\uparrow}}{dxdy} - \frac{d^2\sigma^{\rightarrow\downarrow}}{dxdy} = \frac{8\pi\alpha^2}{q^2}\left(\frac{4M^2x(1-y)}{y(S - M^2)}\right)^{1/2}\left(1 - \frac{M^2xy}{(1-y)(S - M^2)}\right)^{1/2} \times \left[y\, g_1(x, Q^2) + 2g_2(x, Q^2)\right] \quad . \tag{2.49}$$

The charged current induced cross section (2.30) is equal to

$$\frac{d^2\sigma^{(\alpha)}}{dxdy} = \frac{G_F^2}{2\pi}\left(\frac{M_W^2}{M_W^2 + Q^2}\right)^2 (S - M^2)\left[\left\{1 - y - \frac{M^2xy}{S - M^2}\right\} F_2^{(\alpha)}(x, Q^2) + xy^2\, F_1^{(\alpha)}(x, Q^2) - \alpha\, xy(1 - y/2)\, F_3^{(\alpha)}(x, Q^2)\right] \quad . \tag{2.50}$$

3 Calculation of the order α_s^2 corrections to the DIS coefficient functions

In this section we will give an outline of the calculation of the $\mathcal{O}(\alpha_s^2)$ corrections to the deep inelastic (DIS) coefficient functions including their dependence on the renormalization and factorization scales. The underlying assumptions of these calculations in the context of perturbative QCD are the same as those made in the parton model [2]. Here one assumes that in the Bjorken limit ($Q^2 \to \infty, x$ is fixed see (2.41)) the deep inelastic lepton–hadron cross section is given by a sum over the individual lepton parton cross sections. This means that the scattering becomes incoherent and that all interactions between the active parton (the parton which interacts with the lepton) and the spectator partons (the partons which do not interact with the lepton) are neglected. In this way one neglects all power corrections of the type $(m^2/Q^2)^{\tau-2}$ where m^2 is an arbitrary mass scale which is of the order of the confinement scale Λ^2. These power corrections are very often called higher twist terms. In these lectures we will limit ourselves to leading twist ($\tau = 2$) contributions since only in this case there exist very powerful tools like mass factorization, operator product expansion and renormalization group methods which allow us to calculate the QCD corrections up to any order in the strong coupling constant α_s. Expanding the hadronic state denoted by $|p, s>$ in an incoherent sum of parton states $|p_k, s_k>$

$$|p, s >= \sum_k a_k |p_k, s_k > \quad , \tag{3.1}$$

we can write the hadronic tensor $W^{\mu\nu}$ (2.6) or (2.31) as

$$W^{\mu\nu}(p, q, s) = \sum_k |a_k|^2 \hat{W}_k^{\mu\nu}(p_k, q, s_k) \quad , \tag{3.2}$$

where $|a_k|^2$ denotes the probability to find a parton k in the hadron and $\hat{W}_k^{\mu\nu}$ stands for the partonic structure tensor given by

$$\hat{W}_k^{\mu\nu}(p_k, q, s_k) = \frac{1}{4\pi} \int d^4z \; e^{iqz} < p_k, s_k|[j^\mu(z), j^\nu(0)]|p_k, s_k > \quad , \tag{3.3}$$

since the intermediate vector boson V only interacts with the quarks the partonic electroweak current $j^\mu(z)$ is given by

$$j^\mu(z) =: \overline{\Psi}_k(z)\, Q_{k\ell}\, \gamma^\mu\, \Psi_\ell(z) : \quad . \tag{3.4}$$

Here $Q_{k\ell}$ denotes the electroweak charge matrix, Ψ_k is the quark field operator and the symbol ":" stands for normal ordening. The hadronic structure functions listed in (2.41)–(2.43) can now be written as

$$F_i(x, Q^2) = \sum_k |a_k|^2 q_k^2 \; \hat{\mathcal{F}}_{i,k}(z, Q^2) \quad , \tag{3.5}$$

where q_k stands for the electroweak charge and z denotes the Bjorken scaling variable for the parton i.e. $z = Q^2/2p_kq$. Because of the analogy between F_i and $\hat{\mathcal{F}}_{i,k}$ the latter will be called parton structure function. This analogy follows from the property

that the partonic tensor $\hat{W}_k^{\mu\nu}$ in (3.3) can be decomposed in structure functions in the same way as has been done for the hadronic tensors in (2.14) and (2.29). Note that one should not confuse the parton structure function with the parton density which will be defined below. Relation (3.5) also holds for the longitudinal spin structure function $g_1(x, Q^2)$ (2.44) where a_k is now spin dependent. However because of twist three contributions such a simple parton model relation like (3.5) does not exist for the transverse spin structure function $g_2(x, Q^2)$ (2.45). Integrating the probability $|a_k|^2$ over all parton momenta, except for the longitudinal momentum of the struck parton, expression (3.5) can be rewritten as

$$F_i(x, Q^2) = a_i(x) \sum_k q_k^2 \int_x^1 \frac{dz}{z} \hat{f}_k(\frac{x}{z}) \ \hat{\mathcal{F}}_{i,k}(z, Q^2) \quad , \tag{3.6}$$

with

$$a_2(x) = a_3(x) = a_L(x) = x \quad , \qquad\qquad a_1(x) = 1/2 \quad . \tag{3.7}$$

Here $\hat{f}_k(z)$ denotes the parton density. In an infinite momentum frame where both the target hadron as well as the incoming lepton momentum get large (e.g. CM frame lepton–hadron system) the variable z can be interpreted as the fraction of the hadron's momentum carried away by parton k. Notice that only in the case of the scaling parton model [2] where $\hat{\mathcal{F}}_{i,k}$ is given by the Born approximation (see below) the parton densities $\hat{f}_k$ have a physical interpretation. When we include higher order QCD corrections $\hat{\mathcal{F}}_{i,k}$ becomes collinearly divergent so that the latter is unphysical. Since the hadronic structure function $F_i(x, Q^2)$ is an observable quantity we cannot give a physical interpretation to $\hat{f}_k$ anymore. Therefore we will call it the bare parton density indicated by a hat (note the analogy between bare parton density and bare coupling constant and bare masses in renormalized perturbation theory). The radiative corrections to $\hat{\mathcal{F}}_{i,k}$ are computed by using the Feynman rules which are derived from the QCD Lagrangian

$$\mathcal{L}_{QCD} = -\frac{1}{4} F^a_{\mu\nu} F^{a,\mu\nu} + i\overline{\psi}_{i,k} \gamma_\mu D^\mu_{ij} \psi_{j,k} - m_k \overline{\psi}_{i,k} \psi_{i,k} \quad , \tag{3.8}$$

where the gluon field tensor is defined by

$$F^a_{\mu\nu}(x) = \partial_\mu A^a_\nu(x) - \partial_\nu A^a_\mu(x) - g f^{abc} A^b_\mu(x) A^c_\nu(x) \tag{3.9}$$

and the covariant derivative by

$$D^\mu_{ij} = \delta_{ij} \partial^\mu + ig(T^a)_{ij} A^{a,\mu}(x) \quad . \tag{3.10}$$

Here the gluon is described by the gauge field A^a_μ and the quark by the spin half (Dirac) field $\psi_{i,k}$. The Lagrangian in (3.8) is locally gauge invariant under the gauge group $SU(N)_C$ (C=colour) where $N = 3$. The gauge field A^a_μ is put in the adjoint representation which implies that a runs over 1 to $N^2 - 1$. The Dirac field $\psi_{i,k}$ is put in the fundamental representation so that i runs over 1 to N. The generators of the colour gauge group are given by T^a and they satisfy the commutation relations

$$[T^a, T^b] = i f^{abc} T^c \quad , \tag{3.11}$$

where $T^a = T^{a\dagger}$ and $Tr(T^a) = 0$ and f^{abc} denote the structure constants of the Lie-algebra. In the case we can neglect the quark mass m_k the Lagrangian in (3.8) is also globally invariant under $SU(n_f)_F$ (F=flavour) where n_f denotes the number of light flavours. Here the quark field $\psi_{i,k}$ is put in the fundamental representation of the flavour group and k runs over 1 to n_f. Notice that the the gluon field does not carry any flavour index so that it belongs to the flavour singlet representation. If we add the gauge fixing part and the Faddeev-Popov ghost term to the QCD Lagrangian one can quantize the theory and the resulting Feynman rules can be found in the standard text books [30].
The parton structure functions $\hat{F}_{i,k}$ are obtained from the vector boson–parton reaction

$$V(q) + p \to p_1 + p_2 + \cdots p_l \quad . \tag{3.12}$$

Where p is the momentum of the incoming parton k (we drop the index k of p). The ℓ partons in the final state are indicated by their momenta $p_1, \cdots p_l$. Integrating over all parton momenta in the final state (the reaction is inclusive) the parton structure tensor can be written as

$$\hat{W}^{\mu\nu}(p,q,s) = \frac{1}{4\pi}\sum_{\ell=1}^{\infty}\int dPS^{(\ell)} M^{\mu}(\ell) M^{\nu}(\ell)^* \quad , \tag{3.13}$$

where $M^{\mu}(\ell)$ denotes the amplitude of reaction (3.12) and the phase space integral is given by

$$\int dPS^{(\ell)} = \prod_{j=1}^{\ell}\int \frac{d^n p_j}{(2\pi)^{n-1}}\delta^{(+)}(p_j^2)(2\pi)^n\delta^{(n)}(p+q-\prod_{i=1}^{\ell} p_i) \quad . \tag{3.14}$$

Here the partons in the final state are assumed to be massless and the reason that the integrations will be carried out in n dimensions will be explained below. The structure functions $\hat{\mathcal{F}}_{i,k}(i = 1,2,3,L$ and $k = q,g)$ can be extracted from $\hat{W}^{\mu\nu}$ (3.13) via projection methods. Up to order α_s^2 the parton subprocesses which we have calculated are listed in table 1. The corresponding Feynman graphs for the vector boson quark subprocesses are presented in figs. 2-8. The diagrams for the vector boson gluon subprocesses can be obtained from figs. 4,6,7 by interchanging a quark in the initial state with a gluon in the final state. In calculating the loop and phase space integrals one encounters three types of divergences: ultraviolet (UV), infrared (IR) and collinear (C) singularities. Ultraviolet singularities appear because the power of momenta in the numerator of the Feynmann integrals are so large that the latter diverge when the integration (loop) momentum tends to infinity. Infrared and collinear divergences appear when the propagator (denominator) vanishes at some specific value of the momenta over which one is integrating. These singularities are called infrared when they appear if the gluon momentum goes to zero. They are called collinear if they arise when the momentum of an internal parton becomes parallel to an incoming or outgoing parton momentum. The above divergences are cancelled or removed by virtue of the following theorems. Since QCD is a renormalizable theory the UV singularities are removed by replacing the bare coupling constants and bare masses by their renormalized ones (see below). The IR divergences are cancelled by

adding radiative and virtual gluon graphs (Bloch–Nordsieck theorem). The collinear divergences appearing in the final state are also cancelled by adding virtual and radiative graphs because the process is inclusive (Kinoshita–Lee–Nauenberg theorem) The divergences left over, which appear in the parton structure functions $\hat{\mathcal{F}}_{i,k}$ originate from collinear singularities due to initial state interactions They are removed via mass factorization. Notice that the collinear divergences only appear in theories where all particles are massless like in QCD. In the case of QED or the standard model of the electroweak interactions they do not show up because these theories contain a sufficient number of massive particles. The appearance of collinear singularities in QCD is a consequence of the fact that we put the initial state partons on-mass shell so that all long range effects (confinement) are ignored. This is the reason that we can only determine the Q^2–evolution of the hadronic structure functions $F_i(x, Q^2)$ but not their x–dependence. The latter has a non–perturbative origin. Since the appearance of collinear divergences and the mass factorization theorem are characteristic for perturbative QCD we will pay more attention to them than to the UV and IR singularities which removal or cancellation is already treated in the context of the electroweak standard model. Before the above mentioned divergencies are either cancelled or removed they first have to be regularized. For that purpose we have used the technique of n–dimensional regularization which preserves Lorentz covariance and gauge invariance. Notice that for the computation of $\hat{\mathcal{F}}_{3,q}$ and $\hat{g}_{1,q}$ also the γ_5- matrix appears in the traces of the gamma matrices. Since this matrix only exists in four dimensions one has to find a suitable prescription in n dimensions. In our calculations we have adopted the prescription of 't Hooft and Veltman [31] which was elaborated by Breitenlohner and Maison [32]. An explicit calculation of the radiative corrections will not be presented here. For the technicalities in particular the evaluation of the complicated two to three body phase space integrals we refer to the literature [25, 26, 27, 28, 29]. Before discussing the expressions for $\hat{\mathcal{F}}_{i,k}$ and the method of mass factorization we have to distinguish between the singlet and non–singlet part of the structure functions. As an illustration we will limit ourselves to the purely electromagnetic case where Q in (3.4) stands for the charge operator. Using a matrix representation this operator can be expressed into the unit matrix and the generators of the flavour group $SU(n_f)_F$ where n_f stands for the number of light flavours. The generators are denoted by $\lambda_i/2$ which satisfy the same commutation relations as the colour generators T^a in (3.11). Denoting the unit matrix by λ_0 ($n_f \times n_f$ matrix) we have for example

a. $SU(2)_F$ $\quad$ (u, d quarks)

$$Q = \frac{1}{6}\lambda_0 + \frac{1}{2}\lambda_3 \quad , \tag{3.15}$$

$$Q^2 = \frac{5}{18}\lambda_0 + \frac{1}{6}\lambda_3 \quad , \tag{3.16}$$

where λ_3 denotes the third Pauli-matrix.

b. $SU(3)_F$ (u,d,s quarks)

$$Q = \frac{1}{2}\lambda_3 + \frac{1}{2\sqrt{3}}\lambda_8 \quad , \tag{3.17}$$

$$Q^2 = \frac{2}{9}\lambda_0 + \frac{1}{6}\lambda_3 + \frac{1}{6\sqrt{3}}\lambda_8 \quad , \tag{3.18}$$

where λ_3 and λ_8 are the third and eighth Gell-Mann matrices.

c. $SU(4)_F$ $(u, d, s, c$ quarks)

$$Q = \frac{1}{6}\lambda_0 + \frac{1}{2}\lambda_3 + \frac{1}{2\sqrt{3}}\lambda_8 - \frac{1}{\sqrt{6}}\lambda_{15} \quad , \tag{3.19}$$

$$Q^2 = \frac{5}{18}\lambda_0 + \frac{1}{6}\lambda_3 + \frac{1}{6\sqrt{3}}\lambda_8 - \frac{1}{3\sqrt{6}}\lambda_{15} \quad . \tag{3.20}$$

Here λ_i $(i \neq 0)$ denote the generators of $SU(4)_F$. Notice that all λ_i are diagonal. the general expression for Q^2 can be written as

$$Q^2 = \left(\frac{1}{n_f}\sum_{k=1}^{n_f} e_k^2\right)\lambda_0 + A \quad , \tag{3.21}$$

$$A_{ij} = \delta_{ij}\left(e_i^2 - \frac{1}{n_f}\sum_{k=1}^{n_f} e_k^2\right) \quad . \tag{3.22}$$

λ_0 and A are called the singlet and non-singlet (adjoint) parts of the operator Q^2 because they satisfy the relations

$$[\lambda_i, \lambda_0] = 0 \quad , \qquad [\lambda_i, A] \neq 0 \quad , \tag{3.23}$$

where $i = 1 \cdots (n_f^2 - 1)$ $(i \neq 0)$. Inserting the current $j^\mu(z)$ (3.4) in the expression for $\hat{W}_k^{\mu\nu}$ (3.3) we obtain (see also (3.5))

$$F_i \sim \sum_k |a_k|^2 \; < k|Q^2|k > \; \hat{\mathcal{F}}_{i,k} \quad , \tag{3.24}$$

where k runs over all (anti)quarks and the gluon in the initial state. Expression (3.24) can be worked out using (3.21) and (3.22). It becomes equal to

$$\begin{aligned} F_i \quad &\sim |a_g|^2 < g|\lambda_0|g > \left(\frac{1}{n_f}\sum_{k=1}^{n_f} e_k^2\right)\hat{\mathcal{F}}_{i,g} + \\ &\sum_{k=1}^{n_f} |a_k|^2 < k|\lambda_0|k > \left(\frac{1}{n_f}\sum_{\ell=1}^{n_f} e_\ell^2\right)\hat{\mathcal{F}}_{i,q}^S + \sum_{k=1}^{n_f} |a_k|^2 < k|A|k > \hat{\mathcal{F}}_{i,q}^{NS} \quad , \end{aligned} \tag{3.25}$$

where now k only runs over the quarks and anti–quarks. Notice that $\hat{\mathcal{F}}_{i,k}^S$ and $\hat{\mathcal{F}}_{i,k}^{NS}$ are the same for all quarks k independent of the flavour (up, down, strange, charm, etc.)

as long as they are massless. The indices S and NS denote singlet and non–singlet respectively and since the gluon is a flavour singlet we have dropped the superscript S in $\hat{\mathcal{F}}_{i,g}$. Because $|a_k|^2$ corresponds to the parton density $\hat{f}_k$ expression (3.25) can be rewritten as

$$\begin{aligned} F_i \sim & \frac{1}{n_f}\sum_{k=1}^{n_f} e_k^2 \left[\left(\sum_{\ell=1}^{n_f}\hat{f}_\ell\right)\hat{\mathcal{F}}_{i,q}^S + \hat{f}_g\hat{\mathcal{F}}_{i,g}\right] \\ & + \left[\sum_{\ell=1}^{n_f}\left(e_\ell^2 - \frac{1}{n_f}\sum_{k=1}^{n_f} e_k^2\right)\hat{f}_l\right]\hat{\mathcal{F}}_{i,q}^{NS} \quad , \end{aligned} \tag{3.26}$$

If we evaluate this expression for an even number of flavours one obtains

$$\begin{aligned} F_i(x,Q^2) = & a_i(x)\int_x^1 \frac{dz}{z}\left\{\frac{5}{18}\left[\hat{\Sigma}(x/z)\hat{\mathcal{F}}_{i,q}^S(z,Q^2,\epsilon) + \hat{G}(x/z)\hat{\mathcal{F}}_{i,g}(z,Q^2,\epsilon)\right]\right. \\ & \left. + \frac{1}{6}\hat{\Delta}(x/z)\hat{\mathcal{F}}_{i,q}^{NS}(z,Q^2,\epsilon)\right\} \quad , \end{aligned} \tag{3.27}$$

where $a_i(x)$ $(i = 1,2,L)$ is defined in (3.7). Since we will calculate $\hat{\mathcal{F}}_{i,k}$ in higher order of α_s it becomes collinearly divergent and the singularities manifest themselves as pole terms of the type $1/\varepsilon^i$ with $\varepsilon = n-4$ (n–dimensional regularization!!). The gluon density $\hat{g}$, the singlet quark density $\hat{\Sigma}$ and the non–singlet quark density $\hat{\Delta}$ are related to $\hat{f}_k$ in the following way

$$\hat{G}(z) = \hat{f}_g(z) \quad , \tag{3.28}$$

$$\hat{\Sigma}(z) = \sum_q \left(\hat{f}_q(z) + \hat{f}_{\bar{q}}(z)\right) \quad , \tag{3.29}$$

$$\hat{\Delta}(z) = \sum_{q=up}\left(\hat{f}_q(z) + \hat{f}_{\bar{q}}(z)\right) - \sum_{q=down}\left(\hat{f}_q(z) + \hat{f}_{\bar{q}}(z)\right) \quad . \tag{3.30}$$

The expression for the spin structure function $g_1(x,Q^2)$ has the same form as $F_1(x,Q^2)$ where now the densities and the parton structures functions have to be understood in the polarised sense. Proceeding for the neutrino structure function F_i $(i = 2,3)$ in the same way as outlined above one can write in the case of an isoscalar target

$$F_2(x,Q^2) = x\int_x^1 \frac{dz}{z}\hat{\Sigma}(x/z)\hat{\mathcal{F}}_{2,q}^S(z,Q^2,\epsilon) \quad , \tag{3.31}$$

$$F_3(x,Q^2) = x\int_x^1 \frac{dz}{z}\hat{V}(x/z)\hat{\mathcal{F}}_{3,q}^{NS}(z,Q^2,\epsilon) \quad . \tag{3.32}$$

For F_3 we have averaged over the neutrino and the anti–neutrino structure function. The valence quark density which also belongs to the non–singlet class is given by

$$\hat{V}(z) = \sum_q(\hat{f}_q(z) - \hat{f}_{\bar{q}}(z)) \quad . \tag{3.33}$$

We now present the formal expressions of the parton structure functions $\hat{\mathcal{F}}_{i,k}$. In the Born approximation (zeroth order in α_s) they become (see fig.2)

$$\hat{\mathcal{F}}_{L,q}^{(0)} = 0 \quad , \qquad \hat{\mathcal{F}}_{1,q}^{(0)} = \hat{\mathcal{F}}_{2,q}^{(0)} = \hat{\mathcal{F}}_{3,q}^{(0)} = \hat{g}_{1,q}^{(0)} = \delta(1-z) \quad , \qquad \hat{\mathcal{F}}_{3,q}^{(0)} = -\hat{\mathcal{F}}_{3,\bar{q}}^{(0)} \quad , \tag{3.34}$$

$$\hat{\mathcal{F}}^{(0)}_{L,g} = 0 \quad , \qquad \hat{\mathcal{F}}^{(0)}_{1,g} = \hat{\mathcal{F}}^{(0)}_{2,g} = \hat{\mathcal{F}}^{(0)}_{3,g} = \hat{g}^{(0)}_{1,g} = 0 \quad . \tag{3.35}$$

In leading twist the longitudinal structure function $\hat{\mathcal{F}}_{L,k}$ is always zero. The gluonic structure functions $\hat{\mathcal{F}}^{(0)}_{i,g}$, $g^{(0)}_{1,g}$ are zero too because the gluon cannot directly interact with the vector boson V. The relation between $\hat{\mathcal{F}}^{(0)}_{3,q}$ and $\hat{\mathcal{F}}^{(0)}_{3,\bar{q}}$ follows from charge conjugation in the same way as derived for the hadronic structure functions in (2.39) and (2.40) . In the subsequent part of this section we will only present the general form of the expressions for $\hat{\mathcal{F}}_{L,k}$ and $\hat{\mathcal{F}}_{2,k}$ and shortly comment on the other parton structure functions. This general form which our computed expressions have to satisfy follow from the mass factorization theorems derived in [33]. The first order corrections denoted by $\hat{\mathcal{F}}^{(1)}_{i,k}$ have been calculated in the literature at the end of the seventies [18]–[20]. They can be presented in the following from (see figs. 3,4).

$$\hat{\mathcal{F}}^{(1)}_{L,q} = \frac{\alpha^u_s}{4\pi} S_\varepsilon \left(\frac{Q^2}{\mu^2}\right)^{\varepsilon/2} \left[\bar{c}^{(1)}_{L,q} + \varepsilon a^{(1)}_{L,q}\right] \quad , \tag{3.36}$$

$$\hat{\mathcal{F}}^{(1)}_{2,q} = \frac{\alpha^u_s}{4\pi} S_\varepsilon \left(\frac{Q^2}{\mu^2}\right)^{\varepsilon/2} \left[P^{(0)}_{qq}\frac{1}{\varepsilon} + \bar{c}^{(1)}_{2,q} + \varepsilon a^{(1)}_{2,q}\right] \quad , \tag{3.37}$$

$$\hat{\mathcal{F}}^{(1)}_{L,g} = n_f \frac{\alpha^u_s}{4\pi} S_\varepsilon \left(\frac{Q^2}{\mu^2}\right)^{\varepsilon/2} \left[\bar{c}^{(1)}_{L,g} + \varepsilon a^{(1)}_{L,g}\right] \quad , \tag{3.38}$$

$$\hat{\mathcal{F}}^{(1)}_{2,g} = n_f \frac{\alpha^u_s}{4\pi} S_\varepsilon \left(\frac{Q^2}{\mu^2}\right)^{\varepsilon/2} \left[P^{(0)}_{qg}\frac{1}{\varepsilon} + \bar{c}^{(1)}_{2,g} + \varepsilon a^{(1)}_{2,g}\right] \quad . \tag{3.39}$$

The above expressions have to be computed up to terms proportional to ϵ because in the procedure of mass factorization they will be multiplied by $1/\epsilon$. The mass parameter μ, which is an artefact of n–dimensional regularization, originates from the dimensionality of the gauge coupling constant g ($\alpha_s = g^2/4\pi$) in n dimensions. This mass parameter μ should not be confused with the renormalization scale R and the mass factorization scale M which will be introduced later on. The spherical factor S_ϵ, which is also characteristic for n–dimensional regularization is defined by

$$S_\varepsilon = \exp\left\{\frac{\varepsilon}{2}(\gamma_E - \ell n 4\pi)\right\} . \tag{3.40}$$

Further α^u_s denotes the bare strong coupling constant which has to be renormalized later on. Notice that the longitudinal structure functions $\hat{\mathcal{F}}^{(1)}_{L,k}$ do not contain collinear singularities up to $O(\alpha_s)$. The latter show up in $\hat{\mathcal{F}}^{(1)}_{2,k}$. The residues of those singularities are given by the Altarelli–Parisi (AP) splitting functions P_{ij} $(i,j = q,\bar{q},g)$ [6]. Finally there is no distinction between the singlet and non–singlet part of the $\mathcal{O}(\alpha_s)$ contribution to $\hat{\mathcal{F}}_{2,q}$ i.e. $\hat{\mathcal{F}}^{(1),S}_{2,q} = \hat{\mathcal{F}}^{(1),NS}_{2,q}$. The order α_s^2 contributions to $\hat{\mathcal{F}}_{2,q}(z,Q^2,\epsilon)$ take the following form. The non–singlet part is determined by graphs in figs. 5-7 the

contributions A^2, B^2, AB and the term coming from the interference between graphs C and D in fig. 8 (identical quarks in the final state) in. It can be written as

$$\hat{\mathcal{F}}_{L,q}^{(2),\mathrm{NS}} = \left(\frac{\alpha_s^u}{4\pi}\right)^2 S_\varepsilon^2 \left(\frac{Q^2}{\mu^2}\right)^\varepsilon \left[\frac{1}{\varepsilon}\left\{-2\beta_0 \bar{c}_{L,q}^{(1)} + P_{qq}^{(0)} \otimes \bar{c}_{L,q}^{(1)}\right\}\right.$$
$$\left. + \bar{c}_{L,q}^{(2),\mathrm{NS}} - 2\beta_0 a_{L,q}^{(1)} + P_{qq}^{(0)} \otimes a_{L,q}^{(1)}\right] \quad , \tag{3.41}$$

$$\hat{\mathcal{F}}_{2,q}^{(2),\mathrm{NS}} = \left(\frac{\alpha_s^u}{4\pi}\right)^2 S_\varepsilon^2 \left(\frac{Q^2}{\mu^2}\right)^\varepsilon \left[\frac{1}{\varepsilon^2}\left\{\frac{1}{2}P_{qq}^{(0)} \otimes P_{qq}^{(0)} - \beta_0 P_{qq}^{(0)}\right\}\right]$$
$$+ \frac{1}{\varepsilon}\left\{\frac{1}{2}(P_{qq}^{(1),\mathrm{NS}} + P_{q\bar{q}}^{(1),\mathrm{NS}}) - 2\beta_0 \bar{c}_{2,q}^{(1)} + P_{qq}^{(0)} \otimes \bar{c}_{2,q}^{(1)}\right\}$$
$$+ \bar{c}_{2,q}^{(2),\mathrm{NS}} - 2\beta_0 a_{2,q}^{(1)} + P_{qq}^{(0)} \otimes a_{2,q}^{(1)}\Big] \quad , \tag{3.42}$$

where the convolution symbol $\otimes$ is defined by

$$(f \otimes g)(x) = \int_0^1 dx_1 \int_0^1 dx_2 \delta(x - x_1 x_2) f(x_1) g(x_2) \quad . \tag{3.43}$$

The $P_{ij}^{(1)}$ stand for the second order AP splitting functions in the $\overline{\mathrm{MS}}$ -scheme which are computed in [13]-[17]. The coefficients $\bar{c}_{i,k}^{(1)}, a_{i,k}^{(1)}$ already appeared in the $\mathcal{O}(\alpha_s)$ contribution to $\hat{\mathcal{F}}_{i,k}^{(1)}$ (see eqs. (3.36)-(3.39)) and β_0 denotes the lowest order coefficient in the β-function which up to order g^6 is given by

$$\beta(g) = -\beta_0 \left(\frac{g^2}{16\pi^2}\right) - \beta_1 \left(\frac{g^2}{16\pi^2}\right)^2 - \beta_2 \left(\frac{g^2}{16\pi^2}\right)^3 \quad , \tag{3.44}$$

with

$$\beta_0 = \frac{11}{3} C_A - \frac{2}{3} n_f \quad , \tag{3.45}$$

where $C_A = N$ for $SU(N)$ and n_f stands for the number of light flavours. The second coefficient β_1 and the third order coefficient β_2 can be found in [34] and [35] respectively. Notice that the above and subsequent expressions are written in a short hand notation where all arguments in the functions like z, Q^2 are suppressed. Further the non pole terms are constructed in such a way that $\bar{c}_{i,k}^{(l)}$ denotes the order α_s^ℓ contributions to the coefficient functions in the $\overline{\mathrm{MS}}$ -scheme. The pole terms in the second order expressions $\hat{\mathcal{F}}_{i,k}^{(2)}$ originate from collinear as well as ultraviolet singularities since $\hat{\mathcal{F}}_{i,k}^{(2)}$ is proportional to the bare coupling constant. Because there exist two different non-singlet combinations of parton densities $\hat{\Delta}$ (3.30) and $\hat{V}$ (3.32) mass factorization requires that the non-singlet AP splitting function has to be split into (see(3.41))

$$P_{q_i q_j}^{(1),NS} = P_{qq}^{(1),NS} + P_{q\hat{q}}^{(1),NS} \quad . \tag{3.46}$$

We have to do the same for the coefficient function

$$c_{i,q}^{(2),\mathrm{NS}} = c_{i,q}^{(2),\mathrm{NS},+} + c_{i,q}^{(2),\mathrm{NS},-} \quad , \tag{3.47}$$

The last term on the right hand side in (3.46) and (3.47) is due to the presence of identical (anti) quarks in the final state. It originates from the interference between diagrams C and D in fig. 8.
In order α_s^2 the singlet quark parton structure function starts to differ from the non-singlet one. This difference can be traced back to process C in fig. 8 provided the quarks in the final state are not identical. The singlet parton structure function $\hat{\mathcal{F}}_{i,q}^{(S)}$ can be written as

$$\hat{\mathcal{F}}_{i,q}^{(2),\mathrm{S}} = \hat{\mathcal{F}}_{i,q}^{(2),\mathrm{NS}} + \hat{\mathcal{F}}_{i,q}^{(2),\mathrm{PS}} \quad , \tag{3.48}$$

where $\hat{\mathcal{F}}_{L,k}^{(2),\mathrm{NS}}$ and $\hat{\mathcal{F}}_{2,k}^{(2),\mathrm{NS}}$ are presented in (3.41) and (3.42) respectively. The pure singlet part (PS) is given by

$$\hat{\mathcal{F}}_{L,q}^{(2),\mathrm{PS}} = n_f \left(\frac{\alpha_s^u}{4\pi}\right)^2 S_\varepsilon^2 \left(\frac{Q^2}{\mu^2}\right)^\varepsilon \left[\frac{1}{\varepsilon}\left\{P_{gq}^{(0)} \otimes \bar{c}_{L,g}^{(1)}\right\} + \bar{c}_{L,q}^{(2),\mathrm{PS}} + P_{gq}^{(0)} \otimes a_{L,g}^{(1)}\right] \tag{3.49}$$

$$\begin{aligned}\hat{\mathcal{F}}_{2,q}^{(2),\mathrm{PS}} &= n_f \left(\frac{\alpha_s^u}{4\pi}\right)^2 S_\varepsilon^2 \left(\frac{Q^2}{\mu^2}\right)^\varepsilon \left[\frac{1}{\varepsilon^2}\left\{\frac{1}{2}P_{qg}^{(0)} \otimes P_{gq}^{(0)}\right\}\right. \\ &\left. + \frac{1}{\varepsilon}\left\{\frac{1}{2}P_{qq}^{(1),\mathrm{PS}} P_{gq}^{(0)} \otimes \bar{c}_{2,g}^{(1)}\right\} + \bar{c}_{2,q}^{(2),\mathrm{PS}} + P_{gq}^{(0)} \otimes a_{2,g}^{(1)}\right] \quad .\end{aligned} \tag{3.50}$$

In the case the quarks in the final state are identical, we also have to include reactions B and D in fig. 8. However the answers for $\hat{\mathcal{F}}_{i,q}^{(2),\mathrm{NS},+}$ and $\hat{\mathcal{F}}_{i,q}^{(2),\mathrm{PS}}$ do not differ from the ones derived for the non-identical quark case. Note that $\hat{\mathcal{F}}_{i,q}^{(2),\mathrm{NS},+}$ is that part of $\hat{\mathcal{F}}_{i,q}^{(2),\mathrm{NS}}$(3.41), (3.42), which can be attributed to $P_{qq}^{(1),\mathrm{NS}}$ (3.46) and $c_{i,q}^{(2),\mathrm{NS},+}$ (3.47). Finally the order α_s^2 contributions to $\hat{\mathcal{F}}_{i,g}(z, Q^2, \epsilon)$ become

$$\begin{aligned}\hat{\mathcal{F}}_{L,g}^{(2)} &= n_f \left(\frac{\alpha_s^u}{4\pi}\right)^2 S_\varepsilon^2 \left(\frac{Q^2}{\mu^2}\right)^\varepsilon \left[\frac{1}{\varepsilon}\left\{-2\beta_0 \bar{c}_{L,g}^{(1)} + P_{gg}^{(0)} \otimes \bar{c}_{L,g}^{(1)} + P_{qg}^{(0)} \otimes \bar{c}_{L,q}^{(1)}\right\}\right. \\ &\left. + \bar{c}_{L,g}^{(2)} - 2\beta_0 a_{L,g}^{(1)} + P_{gg}^{(0)} \otimes a_{L,g}^{(1)} + P_{qg}^{(0)} \otimes a_{L,q}^{(1)}\right] \quad ,\end{aligned} \tag{3.51}$$

$$\begin{aligned}\hat{\mathcal{F}}_{2,g}^{(2)} &= n_f \left(\frac{\alpha_s^u}{4\pi}\right)^2 S_\varepsilon^2 \left(\frac{Q^2}{\mu^2}\right)^\varepsilon \left[\frac{1}{\varepsilon^2}\left\{\frac{1}{2}P_{qg}^{(0)} \otimes (P_{gg}^{(0)} + P_{qq}^{(0)}) - \beta_0 P_{qg}^{(0)}\right\}\right. \\ &+ \frac{1}{\varepsilon}\left\{\frac{1}{2}P_{qg}^{(1)} - 2\beta_0 \bar{c}_{2,g}^{(1)} + P_{gg}^{(0)} \otimes \bar{c}_{2,g}^{(1)} + P_{qg}^{(0)} \otimes \bar{c}_{2,q}^{(1)}\right\} \\ &\left. + \bar{c}_{2,g}^{(2)} - 2\beta_0 a_{2,g}^{(1)} + P_{gg}^{(0)} \otimes a_{2,g}^{(1)} + P_{qg}^{(0)} \otimes a_{2,q}^{(1)}\right] \quad .\end{aligned} \tag{3.52}$$

The expressions for $\hat{\mathcal{F}}_{1,k}^{(\ell)}$ and $\hat{g}_{1,k}^{(\ell)}$ have the same form as those presented for $\hat{\mathcal{F}}_{2,k}^{(\ell)}$. Notice that in the case of the spin structure function $\hat{g}_1$ the AP splitting functions take their polarized representation which in lowest order can be found in [6]. The

second order contributions $P_{qq}^{(1),S}$ and $P_{qg}^{(1)}$ can be inferred from expressions (3.50) and (3.52) (see [29]). Unfortunately the splitting functions $P_{gq}^{(1)}$ and $P_{gg}^{(1)}$ can only be obtained by performing an order ${\alpha_s}^3$ computation of $\hat{g}_{1,k}$ unless one chooses another method. This problem can be wholly attributed to the fact that the gluon does not directly interact with the virtual vector boson V. For the charged current interactions we have the special properties

$$\hat{\mathcal{F}}_{3,q}^{(\ell),\mathrm{NS}} = -\hat{\mathcal{F}}_{3,\hat{q}}^{(\ell),\mathrm{NS}} \quad , \tag{3.53}$$

$$\hat{\mathcal{F}}_{3,q}^{(\ell),\mathrm{PS}} = \quad \hat{\mathcal{F}}_{3,\bar{q}}^{(\ell),\mathrm{PS}} = 0 \quad , \qquad\qquad \hat{\mathcal{F}}_{3,g}^{(\ell)} = 0 \quad , \tag{3.54}$$

in all orders of perturbation theory and $\hat{\mathcal{F}}_{3,q}^{(\ell),\mathrm{NS}}$ has the same form as $\hat{\mathcal{F}}_{2,q}^{(\ell),\mathrm{NS}}$. The above properties follow from charge conjugation see(2.39) and (2.40). Notice that for $\hat{\mathcal{F}}_{3,\bar{q}}^{(2),\mathrm{NS}}$ the plus sign in eqs. (3.46) and (3.47) has to be replaced by a minus sign. After having computed $\hat{\mathcal{F}}_{i,k}$ we have to perform coupling constant renormalization. Choosing the $\overline{\mathrm{MS}}$ -scheme this can be achieved by replacing the bare (unrenormalized) coupling constant α_s^u by

$$\frac{\alpha_s^u}{4\pi} = \frac{\alpha_s(R^2)}{4\pi}\left(1 + \frac{\alpha_s(R^2)}{4\pi}\frac{2\beta_0}{\varepsilon}S_\varepsilon\left(\frac{R^2}{\mu^2}\right)^{\varepsilon/2}\right) \quad , \tag{3.55}$$

where R represents the renormalization scale. After having removed the UV singularities the remaining pole terms $1/\epsilon^i$ can be attributed to initial state collinear divergences only because $\hat{\mathcal{F}}_{i,k}$ is an inclusive quantity. The latter singularities are removed by mass factorization which proceeds in the following way

$$\hat{\mathcal{F}}_{i,q}^{\mathrm{NS}} = \Gamma_{qq}^{\mathrm{NS}} \otimes C_{i,q}^{\mathrm{NS}} \quad , \tag{3.56}$$

$$\hat{\mathcal{F}}_{i,q}^{\mathrm{S}} = \Gamma_{qq}^{\mathrm{S}} \otimes C_{i,q}^{\mathrm{S}} + \Gamma_{gq} \otimes C_{i,g} \quad , \tag{3.57}$$

$$\hat{\mathcal{F}}_{i,g} = 2n_f\Gamma_{qg} \otimes C_{i,q}^{\mathrm{S}} + \Gamma_{gg} \otimes C_{i,g} \quad . \tag{3.58}$$

In all above quantities coupling constant renormalization has been already carried out so that they all depend on R. The collinear devergences are absorbed in the transition functions Γ_{ij} so that the deep inelastic (DIS) coefficient functions $C_{i,k}$ are finite. Therefore both functions depend on the mass factorization scale M as well as on the coupling constant renormalization R. Since the splitting of eqs. (3.53)–(3.54) in a pole and non–pole part can be done in an arbitrary way (indicated by the scale M) Γ_{ij} and $C_{i,k}$ are scheme dependent. Combining eqs. (3.27) and (3.56)–(3.58) the scale dependent parton densities are defined by

$$\Delta \;=\; \Gamma_{qq}^{\mathrm{NS}} \otimes \hat{\Delta} \quad , \tag{3.59}$$

$$\Sigma \;=\; \Gamma_{qq}^{\mathrm{S}} \otimes \hat{\Sigma} + 2n_f\Gamma_{qg} \otimes \hat{G} \quad , \tag{3.60}$$

$$G \;=\; \Gamma_{gq} \otimes \hat{\Sigma} + \Gamma_{gg} \otimes \hat{G} \quad . \tag{3.61}$$

Contrary to the bare parton densities $\hat{\Delta}$, $\hat{\Sigma}$ and $\hat{g}$ the scale (M) dependent ones, given by Σ, Δ and g, are scheme dependent. In principle the latter also depend on R. However in practice one always chooses $M = R$. Equations (3.57), (3.58) and (3.60), (3.61) can be cast in the form of a matrix equation. The property that the radiative corrections to $\hat{\mathcal{F}}^S_{i,q}$ determine both the gluon and the quark coefficient functions and densities is called mixing. The same holds for the radiative corrections to $\hat{\mathcal{F}}_{i,g}$. This is a special example of a phenomenon characteristic for pertubative calculations in quantum field theory. It states that quantities which belong to the same irreducible representation of an internal and external symmetry group mix under renormalization or mass factorization. Here the quantities $\hat{\mathcal{F}}^S_{i,q}$ and $\hat{\mathcal{F}}_{i,q}$ belong to the flavour singlet representation and therefore mix. The non-singlet representation has one element only i.e. $\hat{\mathcal{F}}^{NS}_{i,q}$ and the mass factorization is simply multiplicative see (3.56)and (3.59). As already mentioned above the functions Γ_{ij} and $C_{i,k}$ are scheme dependent. In the literature there are two popular factorization schemes i.e. the $\overline{\mathrm{MS}}$ -and the DIS-scheme. In these lectures we only present these functions in the $\overline{\mathrm{MS}}$ -scheme. For the DIS-scheme we refer to ([27]). In the $\overline{\mathrm{MS}}$ -scheme the transition functions take the following form.

$$\begin{aligned}\Gamma^{\mathrm{NS}}_{qq} &= 1 + \frac{\alpha^u_s}{4\pi} S_\varepsilon \left(\frac{M^2}{\mu^2}\right)^{\varepsilon/2} \left[\frac{1}{\varepsilon} P^{(0)}_{qq}\right] + \left(\frac{\alpha^u_s}{4\pi}\right)^2 S^2_\varepsilon \left(\frac{M^2}{\mu^2}\right)^{\varepsilon} \\ &\quad \left[\frac{1}{\varepsilon^2}\left\{\frac{1}{2}P^{(0)}_{qq} \otimes P^{(0)}_{qq} - \beta_0 P^{(0)}_{qq}\right\} + \frac{1}{\varepsilon}\left\{\frac{1}{2}P^{(1),\mathrm{NS}}_{qq} + \frac{1}{2}P^{(1),\mathrm{NS}}_{qq}\right\}\right] \quad , \end{aligned} \tag{3.62}$$

$$\Gamma^{\mathrm{S}}_{qq} = \Gamma^{\mathrm{NS}}_{qq} + 2n_f \Gamma^{\mathrm{PS}}_{qq} \quad , \tag{3.63}$$

$$\Gamma^{\mathrm{PS}}_{qq} = \left(\frac{\alpha^u_s}{4\pi}\right)^2 S^2_\varepsilon \left(\frac{M^2}{\mu^2}\right)^{\varepsilon} \left[\frac{1}{\varepsilon^2}\left\{\frac{1}{4}P^{(0)}_{qg} \otimes P^{(0)}_{gq}\right\} + \frac{1}{\varepsilon}\left\{\frac{1}{4}P^{(1),\mathrm{PS}}_{qq}\right\}\right] \quad , \tag{3.64}$$

$$\begin{aligned}\Gamma_{qg} &= \frac{\alpha^u_s}{4\pi} S_\varepsilon \left(\frac{M^2}{\mu^2}\right)^{\varepsilon/2} \left[\frac{1}{2\varepsilon} P^{(0)}_{qg}\right] + \left(\frac{\alpha^u_s}{4\pi}\right)^2 S^2_\varepsilon \left(\frac{M^2}{\mu^2}\right)^{\varepsilon} \left[\frac{1}{\varepsilon^2}\left\{\frac{1}{4}P^{(0)}_{qg}\right.\right. \\ &\quad \left.\left. \otimes \left(P^{(0)}_{gg} + P^{(0)}_{qq}\right) - \frac{1}{2}\beta_0 P^{(0)}_{qg}\right\} + \frac{1}{\varepsilon}\left\{\frac{1}{4}P^{(1)}_{qg}\right\}\right] \quad , \end{aligned} \tag{3.65}$$

$$\Gamma_{gq} = \frac{\alpha^u_s}{4\pi} S_\varepsilon \left(\frac{M^2}{\mu^2}\right)^{\varepsilon/2} \left[\frac{1}{\varepsilon} P^{(0)}_{gq}\right] \quad , \tag{3.66}$$

$$\Gamma_{gg} = 1 + \frac{\alpha^u_s}{4\pi} S_\varepsilon \left(\frac{M^2}{\mu^2}\right)^{\varepsilon/2} \left[\frac{1}{\varepsilon} P^{(0)}_{gg}\right] \quad . \tag{3.67}$$

In order to obtain short expressions we have expressed the transition functions in the bare coupling constant α^u_s. The 1 in (3.62) and (3.67) denotes the distribution $\delta(1-z)$. The same notations holds for the coefficient functions presented below. Further the Γ_{ij} are sufficiently expanded in order α_s to render the coefficient functions finite up to order α^2_s. After having performed coupling constant renormalization (3.55) we

substitute Γ_{ij} into (3.56)–(3.58) and obtain the coefficient functions. Choosing the renormalization scale R to be equal to the mass factorization scale M they read as follows. The non-singlet coefficient function is equal to

$$\bar{C}^{\rm NS}_{L,q} = \frac{\alpha_s}{4\pi}\left[\bar{c}^{(1)}_{L,q}\right] + \left(\frac{\alpha_s}{4\pi}\right)^2 \left[\left\{-\beta_0 \bar{c}^{(1)}_{L,q} + \frac{1}{2}P^{(0)}_{qq} \otimes \bar{c}^{(1)}_{L,q}\right\} L_M + \bar{c}^{(2),{\rm NS}}_{L,q}\right] \quad , \tag{3.68}$$

$$\begin{aligned}\bar{C}^{\rm NS}_{2,q} &= 1 + \frac{\alpha_s}{4\pi}\left[\frac{1}{2}P^{(0)}_{qq} L_M + \bar{c}^{(1)}_{2,q}\right] + \left(\frac{\alpha_s}{4\pi}\right)^2 \left[\left\{\frac{1}{8}P^{(0)}_{qq} \otimes P^{(0)}_{qq} - \frac{1}{4}\beta_0 P^{(0)}_{qq}\right\} L_M^2 \right.\\ &\left. + \left\{\frac{1}{2}\left(P^{(1),{\rm NS}}_{qq} + P^{(1),{\rm NS}}_{q\bar{q}}\right) - \beta_0 \bar{c}^{(1)}_{2,q} + \frac{1}{2}P^{(0)}_{qq} \otimes \bar{c}^{(1)}_{2,q}\right\} L_M + \bar{c}^{(2),{\rm NS}}_{2,q}\right] \end{aligned} \tag{3.69}$$

The singlet coefficient function is given by

$$\bar{C}^{\rm S}_{i,q} = \bar{C}^{\rm NS}_{i,q} + \bar{C}^{\rm PS}_{i,q} \ , \quad (i = 2, L) \ , \tag{3.70}$$

$$\bar{C}^{\rm PS}_{L,q} = n_f \left(\frac{\alpha_s}{4\pi}\right)^2 \left[\left\{\frac{1}{2}P^{(0)}_{gq} \otimes \bar{c}^{(1)}_{L,g}\right\} L_M + \bar{c}^{(2),{\rm PS}}_{L,q}\right] \quad , \tag{3.71}$$

$$\begin{aligned}\bar{C}^{\rm PS}_{2,q} &= n_f \left(\frac{\alpha_s}{4\pi}\right)^2 \left[\left\{\frac{1}{8}P^{(0)}_{qg} \otimes P^{(0)}_{gq}\right\} L_M^2 + \left\{\frac{1}{2}P^{(1),{\rm PS}}_{qq} + \frac{1}{2}P^{(0)}_{gq} \otimes \bar{c}^{(1)}_{2,g}\right\} L_M \right.\\ &\left. + \bar{c}^{(2),{\rm PS}}_{2,q}\right] \ . \end{aligned} \tag{3.72}$$

The gluon coefficient function becomes

$$\begin{aligned}\bar{C}_{L,g} = n_f \frac{\alpha_s}{4\pi}\left[\bar{c}^{(1)}_{L,g}\right] + n_f \left(\frac{\alpha_s}{4\pi}\right)^2 \left[\left\{-\beta_0 \bar{c}^{(1)}_{L,g} + \frac{1}{2}P^{(0)}_{gg} \otimes \bar{c}^{(1)}_{L,g}\right.\right.\\ \left.\left. + \frac{1}{2}P^{(0)}_{qg} \otimes \bar{c}^{(1)}_{L,q}\right\} L_M + \bar{c}^{(2)}_{L,g}\right] \quad , \end{aligned} \tag{3.73}$$

$$\begin{aligned}\bar{C}_{2,g} = n_f \frac{\alpha_s}{4\pi}\left[\frac{1}{2}P^{(0)}_{qg} L_M + \bar{c}^{(1)}_{2,g}\right] + n_f \left(\frac{\alpha_s}{4\pi}\right)^2 \left[\left\{\frac{1}{8}P^{(0)}_{qg} \otimes \left(P^{(0)}_{gg} + P^{(0)}_{qq}\right)\right.\right.\\ \left. - \frac{1}{4}\beta_0 P^{(0)}_{qg}\right\} L_M^2 + \left\{\frac{1}{2}P^{(1)}_{qg} - \beta_0 \bar{c}^{(1)}_{2,g} + \frac{1}{2}P^{(0)}_{gg} \otimes \bar{c}^{(1)}_{2,g}\right.\\ \left.\left. + \frac{1}{2}P^{(0)}_{qg} \otimes \bar{c}^{(1)}_{2,q}\right\} L_M + \bar{c}^{(2)}_{2,g}\right] \quad , \end{aligned} \tag{3.74}$$

where

$$L_M = \ell n \frac{Q^2}{M^2} \quad , \quad \alpha_s \equiv \alpha_s(M^2) \ . \tag{3.75}$$

In the case M is different from R, the resulting coefficient functions can be very easily derived from the above expressions (3.59)–(3.64) by replacing

$$\alpha_s(M^2) = \alpha_s(R^2)\left(1 + \frac{\alpha_s(R^2)}{4\pi}\beta_0 \ell n\left(\frac{R^2}{M^2}\right)\right) \quad . \tag{3.76}$$

The explicit expression for the order-α_s^2 coefficient functions can be found in [25]–[29]. Taking the Mellin transform i.e.

$$C_{i,k}^n(Q^2/M^2) = \int_0^1 dz\, z^{n-1}\, C_{i,k}(z, q^1/M^2) \quad , \tag{3.77}$$

they agree with the results computed for $n = 2, 4, 6, 8, 10$ in [36]. The longitudinal coefficient functions $C_{L,K}$ have been computed earlier in the literature (for a comparison see the discussion in [27, 36]).
Because of the scheme dependence indicated by the scale $M, C_{i,k}$ and Γ_{ij} ($i, j = q, g$, and $k = 1, 2, 3, L$) satisfy renormalization group equations

$$\left[\left(M\frac{\partial}{\partial M} + \beta(g)\frac{\partial}{\partial g}\right)\delta_{kj} - \gamma_{kj}^n\right] C_{i,k}^n(Q^2/M^2) = 0 \quad , \tag{3.78}$$

$$\left[\left(M\frac{\partial}{\partial M} + \beta(g)\frac{\partial}{\partial g}\right)\delta_{kj} + \gamma_{kj}^n\right] \Gamma_{j\ell}^n(\mu^2/M^2) = 0 \quad , \tag{3.79}$$

where $\beta(g)$ is defined in (3.44) and γ_{ij}^n stands for the anomalous dimension of composite operators which is related to the AP splitting functions as follows

$$\gamma_{ij}^{(k),n} = -\int_0^1 dz\; z^{n-1}\, P_{ij}^{(k)} \quad . \tag{3.80}$$

The renormalization group equations can be used to resum the large logarithms L_M when $Q^2 >> M^2$ and to determine the scale dependence of the parton densities (3.59)–(3.61) which follows from (3.79). If γ is a matrix the general solution is quite complicated and we refer to the literature, see e.g. [37]. In the non-singlet case the solution of (3.78) simplifies and we get

$$C_{i,q}^{\mathrm{NS},n}\left(g(M^2), Q^2/M^2\right) = C_{i,q}^{\mathrm{NS},n}\left(\bar{g}(Q^2), 1\right) exp\left\{-\int_{g(M^2)}^{\bar{g}(Q^2)} dx \frac{\gamma^{\mathrm{NS},n}(x)}{\beta(x)}\right\} \quad . \tag{3.81}$$

Here $\bar{g}(Q^2)$ is the running coupling constant ($\bar{g}(M^2) = g(M^2)$) which satisfies the renormalization qroup equation

$$M\frac{d}{dM}\bar{g}(Q^2) = -\beta\left(\bar{g}(Q^2)\right) \quad . \tag{3.82}$$

Solving the above equation up to next to leading order provides us with the well known result ($\bar{\alpha}_s = \bar{g}^2(Q^2)/4\pi$)

$$\frac{\bar{\alpha}_s(Q^2)}{4\pi} = \frac{1}{\beta_0\, \ell n\, \frac{Q^2}{\Lambda^2}} - \frac{\beta_1}{\beta_0}\frac{1}{\left(\beta_0\, \ell n\, \frac{Q^2}{\Lambda^2}\right)^2}\, \ell n\left(\ell n \frac{Q^2}{\Lambda^2}\right) \quad , \tag{3.83}$$

$$\Lambda^2 = M^2 exp\left\{-\frac{4\pi}{\beta_0\alpha_s(M^2)} - \frac{\beta_1}{\beta_0^2}\, \ell n\left(\frac{\beta_0\alpha_s(M^2)}{4\pi}\right)\right\} \quad , \tag{3.84}$$

with $d\Lambda^2/dM^2 = 0$. Using the series expansion for P_{ij} and γ_{ij}

$$\gamma_{ij} = \sum_{m=0}^{\infty}\left(\frac{\alpha_s}{4\pi}\right)^{m+1} \gamma_{ij}^{(m)} \quad , \tag{3.85}$$

we will expand (3.81) up to order $\bar{\alpha}_s^2(Q^2)$. The result becomes for $i = 2, L$

$$
\begin{aligned}
C_{2,q}^{\mathrm{NS},n}(Q^2/M^2) &= B^{\mathrm{NS},n}(M^2)\left[1 + \frac{\bar{\alpha}_s(Q^2)}{4\pi}\left\{c_{2,q}^{(1)} + \frac{\gamma_{qq}^{(1),\mathrm{NS}}}{2\beta_0} - \frac{\beta_1\gamma_{qq}^{(0)}}{2\beta_0^2}\right\}\right. \\
&+ \left(\frac{\bar{\alpha}_s(Q^2)}{4\pi}\right)^2\left\{c_{2,q}^{(2),\mathrm{NS}} + \frac{1}{2}\left(\frac{\gamma_{qq}^{(1),\mathrm{NS}}}{\beta_0} - \frac{\beta_1\gamma_{qq}^{(0)}}{\beta_0^2}\right)c_{2,q}^{(1)}\right. \\
&+ \frac{1}{8}\left(\frac{\gamma_{qq}^{(1),\mathrm{NS}}}{\beta_0} - \frac{\beta_1\gamma_{qq}^{(0)}}{\beta_0^2}\right)^2 \\
&+ \frac{1}{4}\left(\frac{\gamma_{qq}^{(2),\mathrm{NS}}}{\beta_0} - \frac{\beta_1\gamma_{qq}^{(1),\mathrm{NS}}}{\beta_0^2} - \frac{\beta_2\gamma_{qq}^{(0)}}{\beta_0^2} + \frac{\beta_1^2\gamma_{qq}^{(0)}}{\beta_0^3}\right) \\
&\left.\left.\}\right]\left[\bar{\alpha}_s(Q^2)\right]^{\frac{\gamma_{qq}^{(0)}}{2\beta_0}} \quad , \qquad (3.86)
\end{aligned}
$$

$$
\begin{aligned}
C_{L,q}^{\mathrm{NS},n}(Q^2/M^2) &= B^{\mathrm{NS},n}(M^2)\left[\frac{\bar{\alpha}_s(Q^2)}{4\pi}\left\{c_{L,q}^{(1)}\right\} + \left(\frac{\bar{\alpha}_s(Q^2)}{4\pi}\right)^2\left\{c_{L,q}^{(2),\mathrm{NS}}\right.\right. \\
&\left.\left. + \frac{1}{2}\left(\frac{\gamma_{qq}^{(1),\mathrm{NS}}}{\beta_0} - \frac{\beta_1\gamma_{qq}^{(0)}}{\beta_0^2}\right)c_{L,q}^{(1)}\right\}\right]\left[\bar{\alpha}_s(Q^2)\right]^{\frac{\gamma_{qq}^{(0)}}{2\beta_0}} \quad , \qquad (3.87)
\end{aligned}
$$

with

$$
\begin{aligned}
B^{\mathrm{NS},n}(M^2) &= \left[1 - \frac{\alpha_s(M^2)}{4\pi}\left\{\frac{\gamma_{qq}^{(1),\mathrm{NS}}}{2\beta_0} - \frac{\beta_1\gamma_{qq}^{(0)}}{2{\beta_0}^2}\right\}\right. \\
&+ \left(\frac{\alpha_s(M^2)}{4\pi}\right)^2\left\{\frac{1}{8}\left(\frac{\gamma_{qq}^{(1),\mathrm{NS}}}{\beta_0} - \frac{\beta_1\gamma_{qq}^{(0)}}{{\beta_0}^2}\right)^2 - \frac{1}{4}\left(\frac{\gamma_{qq}^{(2),\mathrm{NS}}}{\beta_0}\right.\right. \\
&\left.\left.\left. - \frac{\beta_1\gamma_{qq}^{(1),\mathrm{NS}}}{\beta_0^2} - \frac{\beta_2\gamma_{qq}^{(0)}}{\beta_0^2} + \frac{\beta_1^2\gamma_{qq}^{(0)}}{\beta_0^3}\right)\right\}\right]\left[\bar{\alpha}_s(Q^2)\right]^{\frac{\gamma_{qq}^{(0)}}{2\beta_0}} \quad . \qquad (3.88)
\end{aligned}
$$

Here the n in $\gamma_{qq}^{(l),n}$ has been suppressed. Furthermore one has in lowest order $\gamma_{qq}^{(0),\mathrm{NS}} = \gamma_{qq}^{(0)}$. As we have mentioned before the coefficients $c_{i,q}^{(l)}$ and $\gamma_{qq}^{(l)}$ ($P_{qq}^{(l)}$) are all factorization scheme dependent except for the ones given in lowest order by $c_{L,q}^{(1)}$ (but not $c_{2,q}^{(1)}$) and $\gamma_{qq}^{(0)}$ ($P_{qq}^{(0)}$)). However in the factors multiplying the running coupling constant this scheme dependence is cancelled so that the Q^2–evolution of the coefficient function becomes scheme independent. This phenomenon is one of the nice features of the renormalization group equations (3.78), (3.79). Unfortunately this has as a consequence that the computation of the second order contribution $c_{2,q}^{(2),\mathrm{NS}}$ (3.86) also requires the knowledge of the three–loop (order–α_s^3) contribution to the anomalous dimension given by $\gamma_{ij}^{(2)}$, which can be derived from the the AP splitting function $P_{ij}^{(2)}$. The calculation of the latter, which will be an enormous enterprise, has still to be done. From the renormalization group technique we infer that the

whole factorization scheme dependence of the coefficient functions $C_{2,q}^{NS}$ (3.86) and $C_{L,q}^{NS}$ (3.87) resides in the factor B^{NS} (3.88). This dependence will be cancelled if $C_{k,q}^{NS}$ is multiplied by the non-singlet parton density $\Delta(M^2)$ which satisfies a similar equation as given by (3.79). The latter leads to the following solution.

$$\Delta^n(M^2) = \Delta^n(Q_0^2)\left\{B^{NS,n}(M^2)\right\}^{-1} \quad . \tag{3.89}$$

Here Q_0^2 is some input value for Q^2 at which the parton density is parametrized. Notice that $\Delta(Q_0^2)$ is of a non-perturbative origin so that it cannot be determined by perturbative QCD. Therefore it has to be determined by fitting the non-singlet part of the hadronic structure function, which is given by $(k = 2, L)$

$$F_k^n(Q^2) = \int_0^1 dx\; x^{n-1}\, F_k(x, Q^2) = \frac{1}{6}\Delta^n(M^2) C_{k,q}^{NS,n}\left(Q^2/M^2\right) \quad , \tag{3.90}$$

to the data. Although mathematically the cancellation of the factor $B^{NS,n}$ takes place on the righthand side of (3.90) in practice $(B^{NS,n})^{-1}$ is expanded up to a certain order in α_s $(\alpha_s \equiv \alpha_s(M^2))$ so that in our example

$$\left\{B^{NS,n}(M^2)\right\}\left\{B^{NS,n}(M^2)\right\}^{-1} = a_1\alpha_s^3 + a_2\alpha_s^4 + \ldots \quad . \tag{3.91}$$

Since the coefficients a_i depend on the chosen scheme of $\gamma_{ij}^{(l)}$ $(P_{ij}^{(l)})$ the hadronic structure function will therefore become scheme dependent too. This leads to an M-dependence of $F_k(x, Q^2)$ which is revealed when M is varied between e.g. $Q/2$ and $2Q$. This M-dependence becomes less when higher order-α_s corrections are taken into account. Before finishing this section we want to note that the conclusions drawn from the above analysis of the non-singlet quantitites also apply to the singlet structure functions.

Summarizing the above we have calculated the order α_s^2 contributions to the coefficient functions represented by the coefficients $c_{i,k}^{(2)}$. This calculation has been carried out for light flavours where the mass could be put equal to zero (for heavy flavours see [38]). In order to determine the full Q^2-evolution of the structure functions $F_k(x, Q^2)$ one also needs to know the order-α_s^3 contributions to the AP splitting functions. The calculation of these corrections will be one of the major efforts in the future.

4 Large corrections to the coefficient functions

Before discussing the large corrections to the coefficient functions which are important for the analysis of the hadronic structure functions we want to point out a pecularity which is characteristic for higher order calculations. This is the appearance of the triangular fermion loop in the two loop contribution to $V + q \to q$ (first graph in fig.5) and in the one loop contribution to $V + q \to q + g$ and $V + g \to q + \bar{q}$ (last graph in fig.6). It indirectly also appears in the interference term between the diagrams A and B on the one hand and the diagrams C and D on the other hand. However in this case two fermions are on-shell. This triangular loop only contributes if $V = Z$. In the case of $V = \gamma$ it does not contribute because of Furry's theorem which follows

from charge conjugation (see section 2). A charge conjugation odd state (the photon) cannot couple to a charge conjugation even state (two gluon colour singlet). The same applies to the vector part of $Z-q-q$ interaction. Since a charged particle $V=W^{\pm}$ cannot couple to two neutral gluons this contribution vanishes too. Only the axial vector part of the $Z-q-q$ coupling contributes (charge conjugation even state). The triangular fermion loop graph with the axial vector coupling gives rise to the well known Adler-Bell-Jackiw anomaly which disappears when one sums over all flavours belonging to one family. This implies that for consistency the number of flavours, previously devined by n_f, has to be chosen to be even!! If these flavours are massless the triangular contribution yields zero. However when the flavours are massive like e.g. for bottom and top it provides us with a non zero result which for $m_t \gg m_b$ becomes proportional to $\ln(m_t/m_b)$. notice that this graph does not lead to collinear divergences because in the collinear limit the virtual gluons become on shell and a spin one vector boson (here the Z) cannot couple to two massless helicity one particles (here the gluons). The latter follows from angular momentum conservation (Yang's theorem). The calculation of the coefficient functions $C_{i,k}(z,Q^2/M^2)$ $(z=Q^2/2pq)$ in the last section reveals two types of large corrections appearing at the two extreme values of the scaling variable z i.e. $z\sim 0$ and $z\sim 1$. The large corrections, appearing near the boundary of phase space $z=1$, originate from soft gluon radiation (figs. 4-7) which manifests itself via the large logarithmic terms in the non singlet coefficients

$$\bar{c}_{k,q}^{(i),\mathrm{NS}}(z) \xrightarrow{z\to 1} \sum_{j=0}^{2i-1} a_j^{(i)} \left(\frac{\ell n^j(1-z)}{1-z}\right)_+ \quad , \tag{4.1}$$

or

$$\bar{c}_{k,q}^{(i),\mathrm{NS},n} \xrightarrow{n\to\infty} \sum_{j=0}^{2i-1} \tilde{a}_j^{(i)} \frac{1}{j+1}(\ell n\ n)^{j+1} \quad , \tag{4.2}$$

The above logarithmic terms show up for $k=1,2,3$ and g_1 but not for $k=L$ where they cancel in (2.15). They also show up in the AP splitting functions and in the corresponding anomalous dimensions. However in the $\overline{\mathrm{MS}}$ -scheme they behave themselves in a very mild way.

$$P_{qq}^{(i),\mathrm{NS}}(z) \xrightarrow{z\to 1} a^{(i)} \left(\frac{1}{1-z}\right)_+ \quad , \tag{4.3}$$

or

$$\bar{\gamma}_{qq}^{(i),\mathrm{NS},n} \xrightarrow{n\to\infty} a^{(i)} \ell n\ n \quad , \tag{4.4}$$

The second type of corrections which dominate the $z=0$ region show up in the singlet coefficients

$$\bar{c}_{k,q}^{(i),PS}(z) \xrightarrow{z\to 0} b_{i,q} \frac{\ln^{i-2}(z)}{z} \tag{4.5}$$

$$\bar{c}_{k,g}^{(i)}(z) \xrightarrow{z\to 0} b_{i,g} \frac{\ln^{i-2}(z)}{z} \tag{4.6}$$

for $i \geq 2$ and $k = 1, 2, L$. In the case of the splitting functions the singular behaviour is much more complicate to predict. In any case in all order i they behave like

$$P_{gq}^{(i)} \sim \frac{1}{z} 0(\ln z) \qquad P_{gg}^{(i)} \sim \frac{1}{z} 0(\ln z) \tag{4.7}$$

which is revealed by the lowest order calculations. The above singular behaviour can be traced back to the Bethe-Heitler process in fig.7 and fig. 8 (C,D). In this process the incoming vector boson V decays into a light quark - anti quark pair where one of the (anti) quarks interacts with the incoming gluon or quark via the exchange of multiple gluons in the t-channel. The above singularities originate from the region where all exchanged gluons become soft. The singularities of the type presented in (4.5) - (4.7) are characteristic for the unpolarized coefficient functions and AP splitting functions. They only appear if the incoming gluon or quark helicity is not flipped. In the case of polarized lepton- hadron scattering the helicity has to flip and therefore these type of corrections do not appear in the calculation of the polarized coefficient functions and AP splitting functions. Notice that there exists a similarity between the multiple gluon exchange mechanism and the pomeron exchange in Regge theory. Here the pomeron can only contribute to the unpolarized structure functions whereas it decouples in $g_1(x, Q^2)$

5 Order α_s^2 contributions to the hadronic structure functions

In spite of the fact that the three-loop AP splitting functions $P_{ij}^{(2)}$ are still missing we can still estimate the effect of the order-α_s^2 corrections to the deep inelastic proton structure function which can be wholly attributed to the coefficient function. An exception is the longitudinal structure function where the scheme dependence of the order α_s^2 contribution to the longitudinal coefficient function $C_{L,k}$ is cancelled by the two-loop AP splitting functions $P_{ij}^{(1)}$ $\left(\gamma_{ij}^{(1)}\right)$ which are known [13]–[17] (see expression (3.84)).

The hadronic structure functions follow from (3.26), (3.30), (3.31), the mass factorization formulae (3.53)-(3.55) and the definitions for the parton densities (3.56)-(3.58). They can be expressed into convolution integrals of products of scale dependent parton densities and coefficient functions. In the case $V = \gamma$ we have

$$\begin{aligned} F_i(x, Q^2) = a_i(x) \int_x^1 \frac{dz}{z} \Big\{ \frac{5}{18} \big[\Sigma(x/z, M^2) C_{iq}^S(z, Q^2/M^2) \\ + \quad G(x/z, M^2) C_{i,g}(z, Q^2/M^2) \big] + \frac{1}{6} \Delta(x/z, M^2) C_{i,q}^{NS}(z, Q^2/M^2) \Big\} \end{aligned} \tag{5.1}$$

where $a_i(x)\,(i = 1, 2, L)$ is defined in (3.7). The charged current ($V = W$) hadron structure functions for an isoscalar target are given by

$$F_2(x, Q^2) = x \int_x^1 \frac{dz}{z} \Sigma(x/z, M^2) C_{2,q}^S(z, Q^2/M^2) \tag{5.2}$$

$$F_3(x, Q^2) = x \int_x^1 \frac{dz}{z} V\,(x/z, M^2) C_{3,q}^{NS}(z, Q^2/M^2) \tag{5.3}$$

Here the singlet and non-singlet combination of parton densities, which are denoted by Σ and Δ, V respectively, are defined in the same way as their bare analogues in (3.28), (3.29) and (3.32). The spin structure function $g_1(x, Q^2)$ has the same form as $F_1(x, Q^2)$ where now the parton densities and the coefficient functions are replaced by their polarized expressions [29].
Furthermore we have chosen the mass factorization scale M to be equal to the renormalization scale R. Notice that in all existing parametrizations in the literature for the parton densities one has taken M = R. Our analysis will be carried out in the $\overline{\mathrm{MS}}$ -scheme. The latter has the advantage that the soft gluon corrections occurring in the region $z = 1$ can almost be wholly attributed to the coefficient function (4.1) whereas these corrections show a mild behaviour in the AP splitting functions (4.3). Notice that the latter determine the scale (M) behaviour of the parton densities. Therefore in the limit $x \to 1$ of (5.1)- (5.3) the large corrections to the structure functions are due to the soft gluon corrections to the coefficient function $C_{i,q}(z, Q^2/M^2)$ which dominates the integrand near $z = 1$. The longitudinal structure function receives very small corrections near $x = 1$ because the soft gluon contributions in the corresponding coefficient function $C_{L,q}(z, Q^2/M^2)$ are absent (see the remark below (4.2)). Large corrections to all structure functions also appear in the small x-region which will be explored by the HERA experiments. In the limit $x \to 0$ the integrand in (5.1)-(5.2) either receives large contributions from the region $z \sim x$ where $x/z \sim 1$ or from the region $z = 1$ where $x/z \sim 0$. The region $z \sim x$ is dominated by the singlet and gluonic coefficient functions which show the characteristic behaviour $\frac{1}{z}\,\ell n^i z$ (see (4.5), (4.6)). For $z = 1$ where $x/z \sim 0$ the gluon and sea-quark densities (the latter show up in $\sum(x/z)$) will dominate the integrand because they rise very steeply if $x/z \to 0$ and the coefficient functions behave logarithmically like $\ell n^i(1 - z)$ for $z \to 1$. In practice it will turn out that the analysis of the large corrections near $x = 0$ is much more complicated than that carried out for $x = 1$. It depends very heavily on the parametrization for the parton densities which one has used to compute $F_k(x, Q^2)$. In particular at $z = x$ $(x/z = 1)$ the parton densities tend to zero so that the singular terms $\frac{1}{z}\,\ell n^i z$ in the coefficient functions will be compensated. Therefore the size of the corrections will become very dependent on the behaviour of the parton densities near $z = 1$ $(x/z \sim 0)$. Finally we want to note that the singular terms $\frac{1}{z}\,\ell n^i z$ are absent in the polarized coefficient functions so that in the small x-region $g_1(x, Q^2)$ is rather determined by the gluon or sea quark densities than by the coefficient functions.
The above findings will be illustrated by the plots discussed below. There exist a wealth of parametrizations for the parton densities which are based on past [7] as well as recent [8]–[12] experiments. The parton densities are either computed by the inverse Mellin transformation of (3.86) or via the Altarelli-Parisi equations [6] which follow from the renormalization group equations in (3.75), (3.76). In the plots we will use the following set of parton densities which are corrected up to next to leading

order (NL0) $\overline{\text{MS}}$ -scheme)

a. MTB1-MS , Table I_4–FIT B1 - MS, $\Lambda = 0.190$ GeV [39]

b. MTB2-MS , Table I_6–FIT B2 - MS, $\Lambda = 0.191$ GeV [39]

c. HMRSB , $\Lambda = 0.190$ GeV [40]

d. MRS (D0) , $\Lambda = 0.215$ GeV [41]

e. MRS (D–) , $\Lambda = 0.215$ GeV [41]

where n_f is chosen to be four in the densities as well as in the coefficient functions. Here the MTB2-MS and the MRS (D–) parametrizations are characterized by the steeply rising behaviour of the gluon and sea quark densities near $z = 0$ i.e. $z\,G(z) \sim z^{-1/2}, zs(z) \sim z^{-1/2}$ (Lipatov pomeron). Furthermore we use the two-loop corrected running coupling constant (3.80) with $n_f = 4$ and the same Λ (3.81) as in $a - e$. Finally we put the factorization scale $M^2 = Q^2$. For other choices of M see [27].
In order to investigate the effect of the $\mathcal{O}(\alpha_s^2)$ correction to the coefficient functions on the hadronic structure function $F_2(x, Q^2)$ (5.1) we plot the ratio

$$K^{(2)}(x, Q^2) = \frac{F_2^{(2)}(x, Q^2)}{F_2^{(1)}(x, Q^2)} \tag{5.4}$$

Here $F_i^{(n)}(x, Q^2)$ denotes the structure function which contains the NL0 parton densities and the coefficient functions are corrected up to $\mathcal{O}(\alpha_s^n)$. Note that in principle for $F_2^{(2)}(x, Q^2)$ the NNL0 parton densities should be used but they are not available since the AP splitting functions are not known up to $\mathcal{O}(\alpha_s^3)$. The NL0 parton densities are determined in such a way that $F_2^{(1)}(x, Q^2)$ fits the data. The deviation of $K^{(2)}$ from one will then indicate how the free (non-perturbative) parameters describing the z-dependence of the parton densities have to be modified in order to bring $F_2^{(2)}(x, Q^2)$ in agreement with the data. In fig. 9 we have plotted $K^{(2)}$ for various Q^2–values in the range $10^{-4} < x < 1$. The corrections for $x > 0.5$ are large and positive which can be attributed to soft gluon radiation. The corrections in the small x-region ($x < 0.01$) which are negative can be attributed to the second order gluonic coefficient $\bar{c}_{2,g}^{(2)}(z)$. The corrections get smaller, when Q^2 increases due to the effect of the running coupling constant. We do not expect that this picture will be altered when the three-loop AP non-singlet splitting functions $P_{ij}^{(2)}$ are included except for the small x-region where the calculation of this missing contribution will be necessary. The dependence of $K^{(2)}$ on the various parametrization for the parton densities is shown in fig. 10 for $Q^2 = 10$ GeV^2. The figure reveals that the parametrization with the steepest behaviour of the gluon density provides us with the smallest correction. Since the sea quark density is correlated with the gluon density there must be a cancellation in the singlet part of $F_2^{(2)}(x, Q^2)$ due to the opposite signs of $c_{2,q}^{(2)}$ and $c_{2,g}^{(2)}$.
We now focus our attention on the effect of the order–α_s^2 correction to the longitudinal structure function $F_L(x, Q^2)$. In particular we are interested in the ratio of

the longitudinal and transverse cross section defined by $R = \sigma_L/\sigma_T$. The order α_s^n corrected R denoted by $R^{(n)}$ is given by

$$R^{(n)}(x,Q^2) = \frac{F_L^{(n)}(x,Q^2)}{\left(1+\frac{4M_p^2x^2}{Q^2}\right) F_2^{(n-1)}(x,Q^2) - F_L^{(n)}(x,Q^2)} \tag{5.5}$$

where M_p stands for the proton mass. In fig. 11 we have plotted $R^{(2)}$ in the range $10^{-4} < x < 1$ for various Q^2–values and the chosen set MRS(D0). The figure reveals that $R^{(2)}$ is very small in the large x-region ($0.1 < x < 1$). When x gets smaller $R^{(2)}$ increases very rapidly and then flattens out. Further we observe a turning point at $x = 0.001$. On the left-hand side of this point $R^{(2)}$ increases when Q^2 gets larger whereas on the right-hand side $R^{(2)}$ decreases when Q^2 grows. In fig. 12 we have compared $R^{(1)}$ with $R^{(2)}$ for the same parton density set as in fig. 11. In the small x-region the lowest order term $R^{(1)}$ gets very negative corrections ($\sim -50\%$) which is due to the second order gluonic coefficient $c_{L,g}^{(2)}$. The reason that the gluonic coefficient function has a much larger effect on F_L than on F_2 can be attributed to its absence on the Born level in the case of F_L. In fig. 13 we studied the sensitivity of $R^{(1)}$ and $R^{(2)}$ on the input parton density set. Here we compared MRS (D0) with MRS (D–) [41] where the latter contains the steeply rising gluon density near $z = 0$. The figure shows a strong dependence on the two different parametrizations in particular in the small x-region. The result obtained from MRS (D–) lies significantly above the one given by MRS (D0). The difference becomes even larger when higher order QCD corrections are included(compare $R^{(1)}$ (D–) - $R^{(1)}$ (D0) with $R^{(2)}$ (D–) - $R^{(2)}$ (D0). In the case of MTB2 (see [27]) which also contains a steeply rising gluon density we observe a completely different picture. First $R^{(n)}$ (MTB2-MS) $< R^{(n)}$ (MRS(D0)) ($n = 1,2$) and second the gap between both becomes less when higher order corrections are taken into account. Therefore R provides us with a beautiful quantity to measure the still unknown gluon density in the small z-region. For large x-values i.e. $x > 0.1$ the various parton densities predict the same R which is in agreement with the BCDMS data [10] (fig. 14). In this region the $\mathcal{O}(\alpha_s)$ corrections turn out to be small. In fig. 15 we have presented the $\mathcal{O}(\alpha_s)$ corrected and the $\mathcal{O}(\alpha_s^2)$ corrected charged current structure function denoted by $F_3^{(1)}(x,Q^2)$ and $F_3^{(2)}(x,Q^2)$ respectively. Since the target is an isoscalar $F_3(x,Q^2)$ is purely non–singlet. The figure shows that the $\mathcal{O}(\alpha_s^2)$ corrections are small and they lie within the range given by the mass factorization scale variation of $F_3^{(1)}(x,Q^2)$ i.e. $Q/2 < M < 2Q$. We do not expect that the still missing three loop AP splitting function will appreciably alter this picture since it is supposed to be small in the $\overline{\text{MS}}$ –scheme. The same picture also holds for the charged current structure function $F_2(x,Q^2)$ (see [28]).

As a last application of our calculations we call attention to the higher order corrections to the spin structure function $g_1(x,Q^2)$ which has the same form as $F_1(x,Q^2)$ in (5.1). Taking the Mellin transform (n^{th} moment it becomes equal to

$$\begin{aligned} g_1^n(Q^2) &= \int_0^1 dx\, x^{n-1} g_1(x,Q^2) = \frac{1}{2}\left[\frac{5}{18}\left\{\Sigma^n(M^2)C_q^{S,n}\left(Q^2/M^2\right)\right.\right. \\ &+ \left.\left. G^n(M^2)C_g^n\left(Q^2/M^2\right)\right\} + \frac{1}{6}\Delta^n(M^2)C_q^{NS,n}\left(Q^2/M^2\right)\right] , \end{aligned} \tag{5.6}$$

The first moment ($n = 1$) represents the Ellis-Jaffe sum rule [42]. Experiments have shown [43, 44] that the measured sum rule is below the theoretical zeroth order prediction which is based on the constituent quark model (see [42]). This discrepancy came as a great surprise because one expected that sum rules corresponding to conserved quantities, which are derived in the context of the constituent quark model at low energy scales, would also be valid at large energy scales characteristic for the current (parton) quark regime. Notice that sum rules which correspond to conserved quantities do not show scaling violating effects dus to QCD corrections. This implies that the anomalous dimensions defined in (3.77) for $n = 1$, which rule the scale evolution M of the parton densities, are zero. This principle, which seems to work for unpolarized quantities is apparently violated in the polarized case.
Many theorists have tried to explain the above discrepancy, for reviews see [45, 46]. One of the issues was the question whether the experimental result for the Ellis-Jaffe sum rule, which turned out to be much smaller than expected, can either be explained by a large positive polarized gluon density or by a large negative polarized sea-quark density inside the proton, although a combination of both is also possible. Here we adopt the point of view advocated in [33, 47] that the above parton densities which were used to explain the measured size of the sum rule depend on the mass factorization scheme chosen for the polarized AP splitting functions and the polarized coefficient functions. From (5.6) we infer that the gluon density can only contribute if higher order QCD corrections are taken into account in particular the gluonic coefficient function C_g. The sea quark density enters via Σ already on the lowest order level. Notice that C_q^S on the Born level is non–vanishing. Unfortunately in the $\overline{\mathrm{MS}}$ -scheme the first moment of C_g i.e. C_g^1 vanishes in all orders of perturbation theory which is confirmed by our calculations up to $\mathcal{O}(\alpha_s^2)$. Therefore in this scheme the large negative correction, necessary to bring (5.6) in agreement with the data can be only achieved by a negative polarized sea quark density. Using the parametrization for the polarized parton densities in [48] we have shown the $\mathcal{O}(\alpha_s^k)$ corrected structure function denoted by $g_1^{(k)}(x, Q^2)$ for $Q^2 = 10$ GeV^2 in fig. 16. The figure reveals that the $\mathcal{O}(\alpha_s)$ and $\mathcal{O}(\alpha_s^2)$ corrections are very small and all lie between the error bars of the data in [43, 44]. In fig. 17 we have shown the Q^2-evolution of $g_2(x, Q^2)$, which is hardly noticeable. Apart form the vanishing of C_g^1 the $\overline{\mathrm{MS}}$ -scheme also entails the nonvanishing of the first moment of the singlet anomalous dimension $\gamma_{qq}^{S,1}$ up to second order. This means that the conservation of the singlet quark helicity is broken at the two loop level.
Therefore some theorists prefer a scheme where $\gamma_{qq}^{S,1} = 0$ and $C_g^1 < 0$. The latter value requires a large positive gluon density to bring the Ellis–Jaffe sum rule in agreement with experiment. Choosing the last scheme and the gluon density in [48] we have plotted $g_1^{(k)}(x, Q^2)$ for $k = 0, 1, 2$ and $Q^2 = 10$ GeV^2 (see fig. 18). The zeroth order result, where the sea quark density is put equal to zero, is the original prediction of Ellis and Jaffe [42]. The correction due to the gluonic part of (5.6) is large and negative. The $\mathcal{O}(\alpha_s^2)$ corrections hardly modify the $\mathcal{O}(\alpha_s)$ corrected structure function. In the case of a large gluon density we also observe an appreciable Q^2-evolution in $g_1(x, Q^2)$ (see fig. 19) which will be detected when higher statics data become available. Hopefully they will be obtained by future experiments [23, 24]. A sum rule

which is from the theoretical point of view even more fundamental than the Ellis-Jaffe one is given by Bjorken in [49]. It originates from the non-singlet part of (5.6). For $n = 1$ we get (p = proton, n = neutron).

$$g^1_{1,p}(Q^2) - g^1_{1,n}(Q^2) = \frac{1}{6}\Delta^1(M^2)C_q^{NS,1}(Q^2/M^2) \tag{5.7}$$

Recently the above sum rule is confirmed by the EMC experiment [50]. A recent measurement of the Bjorken sum rule is done by the E142 experiment at SLAC [51]. Here one finds a value which is lower (two σ effect) than the one theoretically predicted.

References

[1] D.H. Coward et al., Phys. Rev. Lett. 20 (1968) 292;
E.D. Bloom et al., Phys. Rev. Lett. 23 (1969) 930;
H. Breidenbach et al., Phys. Rev. Lett. 23 (1969) 935.

[2] R.P. Feynman, "Photon-Hadron Interactions", W.A. Benjamin, New York 1972.

[3] H. Fritsch, M. Gell-Mann and H. Leutwyler, Phys. Lett. B74 (1973) 365,
W. Marciano and H. Pagels, Phys. Rep. 36C (1978) 137.

[4] K. Wilson, Phys. Rev. D10 (1974) 2455.

[5] D.J. Gross and F. Wilczek, Phys. Rev. Lett. 30 (1973) 1343;
H.D. Politzer,Phys. Rev. Lett. 30 (1973) 1346.

[6] V.N. Gribov and L.N. Lipatov, Sov.J.Nucl.Phys. 15 (1972)438, 675;
G. Altarelli and G. Parisi, Nucl. Phys. B126 (1977) 298.

[7] R.G. Roberts and M.R. Whalley, J. Phys. G.; Nucl. Part. Phys. 17 (1991) D1-D151.

[8] I.J. Aubert et. al. (EMC), Nucl. Phys. B293 (1987) 740.

[9] J.P. Berge et. al. (CDHSW), Z. Phys. C49 (1990) 187.

[10] A.C. Benvenuti et. al. (BCDMS), Phys. Lett. B223 (1989) 485; ibid. B237 (190) 599.

[11] E. Oltman et. al. (CCFR), Z. Phys. C53 (1992) 51.

[12] P. Amaudruz et. al. (NMC), Nucl. Phys. B371 (1992) 3.

[13] E.G. Floratos, D.A. Ross and C.T. Sachrajda, Nucl. Phys. B129 (1977) 66, Erratum B139 (1978) 545; Nucl.Phys. B152 (1979) 493.

[14] A. Gonzalez-Arroyo, C. Lopez and F.J. Yndurain, Nucl. Phys. B153 (1979) 161.

[15] A. Gonzalez-Arroyo and C. Lopez, Nucl. Phys. B166 (1980) 429.

[16] E.G. Floratos, P. Lacaze and C. Kounnas, Phys. Lett. B98 (1981) 89, 225.

[17] G. Curci, W. Furmanski and R. Petronzio, Nucl. Phys. B175 (1980) 27; W. Furmanski and R. Petronzio, Phys. Lett. B97 (1980) 437.

[18] W.A. Bardeen, A.J. Buras, D.W. Duke and T. Muta, Phys.Rev. D18 (1978) 3998.

[19] G. Altarelli, R.K. Ellis and G. Martinelli, Nucl. Phys. B143 (1978) 521, Erratum B146 (1978) 544; ibid. B157 (1979) 461.

[20] B. Humpert and W.L. van Neerven, Nucl. Phys. B184 (1981) 225.

[21] Proceedings of the Workshop "Physics at HERA", vols. 1,2,3. Hamburg, October 29-30, 1991. Edited by W. Buchmüller and G. Ingelman.

[22] Proceedings of the Large hadron Collider Workshop, vol. 2 p. 829. Aachen, October 4–9, 1990. Edited by G. Jarlskog and D. Rein.

[23] J. Beaufays et. al. (SMC), CERN/SPSC 88-47, SPSC/p.242 (1988).

[24] M. Düren and K. Rith, "Polarized Electron–Nucleon–Scatterng at HERA. The HERMES Experiment". Proceedings of the workshop "Physics of HERA", vo. 1, p. 427. Hamburg, October 29-30, 1991. Edited by W. Buchmüller and G. Ingelman.

[25] W.L. van Neerven and E.B. Zijlstra, Phys. Lett. B272 (1991) 127.

[26] E.B. Zijlstra and W.L. van Neerven, Phys. Lett. B273 (1991) 476.

[27] E.B. Zijlstra and W.L. van Neerven, Nucl. Phys. B383 (1992) 525.

[28] E.B. Zijlstra and W.L. van Neerven, Phys. Lett. B297 (1992) 377.

[29] E.B. Zijlstra and W.L. van Neerven, Leiden preprint, INLO–PUB–3/93

[30] D. Bailin and A. Love, "Introduction to Gauge Field Theory". Adam Hilger
L. Ryder, "Quantum Field Theory", Cambridge Univ. Press.
C. Itzykson and J.B. Zuber, "Quantum Field Theory" , Mc. Graw-Hill.

[31] G. 't Hooft and M. Veltman, Nucl. Phys. B44 (1972) 189.

[32] F. Breitenlohner and D. Maison, Commun. Math. Phys. 52 (1977) 11, 39, 55

[33] J.C. Collins, Nucl. Phys. B394 (1992) 169 and references therein.

[34] D.R.T. Jones, Nucl. Phys. B75 (1974) 531

[35] O.V. Tarasov, A.A. Vladimirov and A.Yu. Zharkov, Phys. Lett. B93 (1980) 429

[36] S.A. Larin and J.A.M Vermaseren, Z. Phys. C57 (1993) 93.

[37] A.J. Buras, Rev. Mod. Phys. 52 (1980) 199.

[38] E. Laenen, S. Riemersma, J. Smith and W.L. van Neerven, Nucl. Phys. B392 (1993) 162, 229.

[39] J.G. Morfin and Wu-Ki Tung, Z. Phys. C52 (1991) 13.

[40] P.N. Harriman, A.D. Martin, R.G. Roberts and W.J. Stirling, Phys. Rev. D42 (1990) 798.

[41] A.D. Martin, W.J. Stirling and R.G. Roberts, DTP–92–16, RAL–92–021, 1992.

[42] J. Ellis and R. Jaffe, Phys. Rev. D9 (1974) 1444; ibid. D10 (1974) 1669

[43] M.J. Alguard et. al. (SLAC), Phys. Rev. Lett. 37 (1978) 1262, ibid. 46 (1978) 70.
G. Baum et. al. (SLAC), Phys. Rev. Lett. 51 (1983) 1135.

[44] J. Ashman et. al. (EMC), Phys. Lett. B206 (1988), Nucl. phys. B328 (1989) 1.

[45] G. Altarelli, "Polarized Structure Functions at HERA, Introduction and Overview", Proceedings of the Workshop: Physics at HERA, Hamburg, October 29–30, 1991, eds. W. Buchmüller and G. Ingelman, vol. 1, p. 379.

[46] E. Reya, Dortmund preprint DO-TH 92/17

[47] G.T. Bodwin and J. Qiu, Phys. Rev. D41 (1990) 2755.

[48] Hai-Yang Cheng and C.F. Wai, Phys. Rev. D46 (1992) 125

[49] J.D. Bjorken, Phys. Rev. 148 (1966) 1467, Phys. Rev D1 (1970) 1376

[50] B. Adeva et. al., Phys. Lett. B302 (1993) 533.

[51] R. Arnold et. al. (E142), SLAC proposal, unpublished.

Figure captions

Fig. 1 Kinematics of the deep inelastic process $l_1 + H \to l_2 + "X"$.

Fig. 2 The Born contribution to the subprocess $\mathrm{q}(\overline{\mathrm{q}}) + V \to \overline{\mathrm{q}}(\mathrm{q})$.

Fig. 3 The one loop correction to the subprocess $\mathrm{q}(\overline{\mathrm{q}}) + V \to \overline{\mathrm{q}}(\mathrm{q})$.

Fig. 4 Diagrams contributing to the subprocess $\mathrm{q}(\overline{\mathrm{q}}) + V \to \mathrm{q}(\overline{\mathrm{q}}) + \mathrm{g}$. The graphs corresponding to the subprocess $\mathrm{g} + V \to \mathrm{q} + \overline{\mathrm{q}}$ can be obtained from those presented in this figure by interchanging the incoming (anti)quark line with the outgoing gluon line.

Fig. 5 The two loop corrections to the subprocess $\mathrm{q}(\overline{\mathrm{q}}) + V \to \mathrm{q}(\overline{\mathrm{q}})$. The ghost contribution to the gluon self energy is included but not shown in the figure.

Fig. 6 The one loop corrections to the subprocess $q(\bar{q}) + V \to q(\bar{q}) + g$. The graphs corresponding to the subprocess $g + V \to q + \bar{q}$ can be obtained from those presented in this figure by interchanging the incoming (anti)quark line with the outgoing gluon line.

Fig. 7 Diagrams contributing to the subprocess $q(\bar{q}) + V \to q(\bar{q}) + g + g$. The graphs corresponding to the subprocess $g + V \to g + q + \bar{q}$ can be obtained from those presented in this figure by interchanging the incoming (anti)quark line with one of the outgoing gluon lines.

Fig. 8 Diagrams contributing to the subprocesses $q + V \to q(1) + q(2) + \bar{q}$ and $\bar{q} + V \to \bar{q}(1) + \bar{q}(2) + q$. If $q(1) \neq q(2)$ or $\bar{q}(1) \neq \bar{q}(2)$, only combinations A and C have to be considered. If $q(1) = q(2)$ or $\bar{q}(1) = \bar{q}(2)$, combinations B and D have to be added to A and C.

Fig. 9 The quantity $K^{(2)}(x, Q^2)$ (5.4) (MTB1MS) in the region $0.01 < x < 0.9$ for $Q^2 = 10$ GeV^2 (solid line), $Q^2 = 100$ GeV^2 (dashed line) and $Q^2 = 10^4$ GeV^2 (dashed dotted line) and in the region $10^{-4} < x < 10^{-2}$ for $Q^2 = 10$ GeV^2 (solid line), $Q^2 = 50$ GeV^2 (dashed line) and $Q^2 = 100$ GeV^2 (dashed dotted line).

Fig. 10 Structure function dependence of $K^{(2)}(x, Q^2)$ at $Q^2 = 10$ GeV^2 in the region $10^{-4} < x < 0.9$: MTB1MS (solid line), MTB2MS (dashed line), HMRSB (dashed dotted line).

Fig. 11 The quantity $R^{(2)}(x, Q^2)$ (5.5) (MRS(D0)) in the region $0.01 < x < 0.9$ for $Q^2 = 10$ GeV^2 (solid line), $Q^2 = 100$ GeV^2 (dashed line) and $Q^2 = 10^4$ GeV^2 (dashed dotted line) and in the region $10^{-4} < x < 10^{-2}$ for $Q^2 = 10$ GeV^2 (solid line), $Q^2 = 50$ GeV^2 (dashed line) and $Q^2 = 100$ GeV^2 (dashed dotted line).

Fig. 12 The quantity $R^{(i)}(x, Q^2)$ (5.5) (MRS(D0)) at $Q^2 = 10$ GeV^2 in the region $10^{-4} < x < 0.9$: $R^{(1)}(x, Q^2)$ (solid line), $R^{(2)}(x, Q^2)$ (dashed line) and $R^{(3)}(x, Q^2)$ (dashed dotted line).

Fig. 13 Parton density dependence of $R^{(i)}(x, Q^2)$ (5.5) at $Q^2 = 10$ GeV^2 in the region $10^{-4} < x < 0.9$: $R^{(1)}(x, Q^2)$ (MRS(D0), solid line), $R^{(2)}(x, Q^2)$ (MRS(D0), short dashed line), $R^{(1)}(x, Q^2)$ (MRS(D-), dotted line), $R^{(2)}(x, Q^2)$ (MRS(D-), long-dashed line).

Fig. 14 Comparison of $R^{(i)}(x, Q^2)$ (5.5) (MRS(D0)) with the BCDMS data ([10]) : $R^{(1)}(x, Q^2)$ (dashed dotted line), $R^{(2)}(x, Q^2)$ (solid line).

Fig. 15 Factorization scale dependence of $F_3^{(1)}(x, Q^2)$ and a comparison with $F_3^{(2)}(x, Q^2)$. Dotted line: $F_3^{(1)}(x, Q^2)$, $M = \frac{1}{2}Q$. Solid line: $F_3^{(1)}(x, Q^2)$, $M = Q$. Short–dashed line: $F_3^{(1)}(x, Q^2)$, $M = 2Q$. Long–dashed line: $F_3^{(2)}(x, Q^2)$, $M = Q$.

Fig. 16 The order–α_s^k corrected spin structure function $xg_1^{(k)}(x, Q^2)$. The parton densities are obtained from ([48]) with a large negative polarized sea quark

density and the gluon density equals zero. $M^2 = Q^2 = 10$ GeV^2; solid line: $xg_1^{(0)}(x, Q^2)$; dotted line: $xg_1^{(1)}(x, Q^2)$; short–dashed: $xg_1^{(2)}(x, Q^2)$; The data are obtained from ([44]).

Fig. 17 The Q^2–dependence of the order $-\alpha_s^2$ corrected spin structure function $xg_1^{(2)}(x, Q^2)$. The parton densities are the same as mentioned in fig. 16. $M^2 = 10$ GeV^2. Solid line: $Q^2 = 10$ GeV^2; dotted line: $Q^2 = 50$ GeV^2; short–dashed line: $Q^2 = 100$ GeV^2. The data are obtained from ([44]).

Fig. 18 The same as in fig. 16 but now with a large positive polarized gluon density and the sea quark density is set equal to zero.

Fig. 19 The same as in fig. 17 but now with the parton densities used in fig. 18.

DIS subprocesses				
α_s^0:	$V + q(\overline{q})$	$\rightarrow$	$q(\overline{q})$	
α_s^1:	$V + q(\overline{q})$	$\rightarrow$	$q(\overline{q})$	(one loop correction)
	$V + q(\overline{q})$	$\rightarrow$	$q(\overline{q}) + g$	
	$V + g$	$\rightarrow$	$q + \overline{q}$	
α_s^2:	$V + q(\overline{q})$	$\rightarrow$	$q(\overline{q})$	(two loop correction)
	$V + q(\overline{q})$	$\rightarrow$	$q(\overline{q}) + g$	(one loop correction)
	$V + q(\overline{q})$	$\rightarrow$	$q(\overline{q}) + g + g$	
	$V + q(\overline{q})$	$\rightarrow$	$q(\overline{q}) + q(\overline{q}) + \overline{q}(q)$	
	$V + g$	$\rightarrow$	$q + \overline{q}$	(one loop correction)
	$V + g$	$\rightarrow$	$q + \overline{q} + g$	

Table 1. List of deep inelastic lepton-parton subprocesses up to $\mathcal{O}(\alpha_s^2)$.

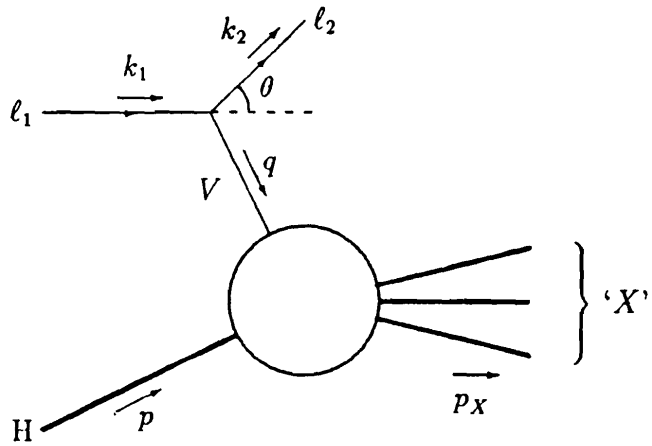

Fig. 1

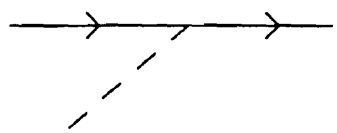

Fig. 2

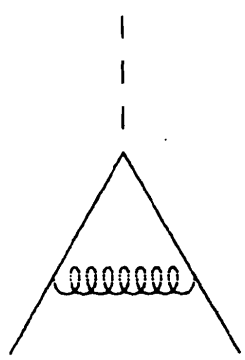

Fig. 3

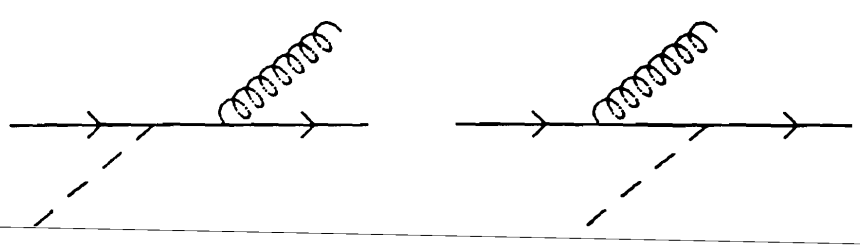

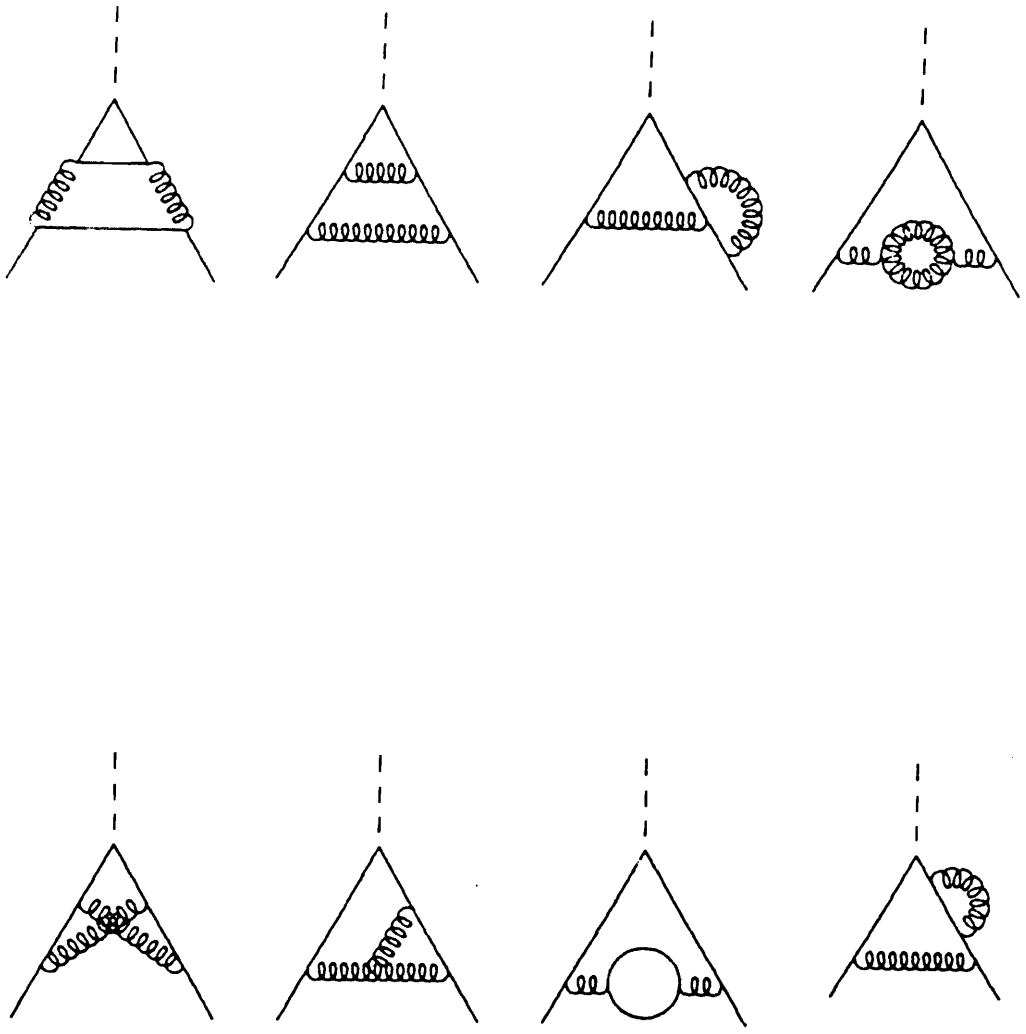

Fig. 5

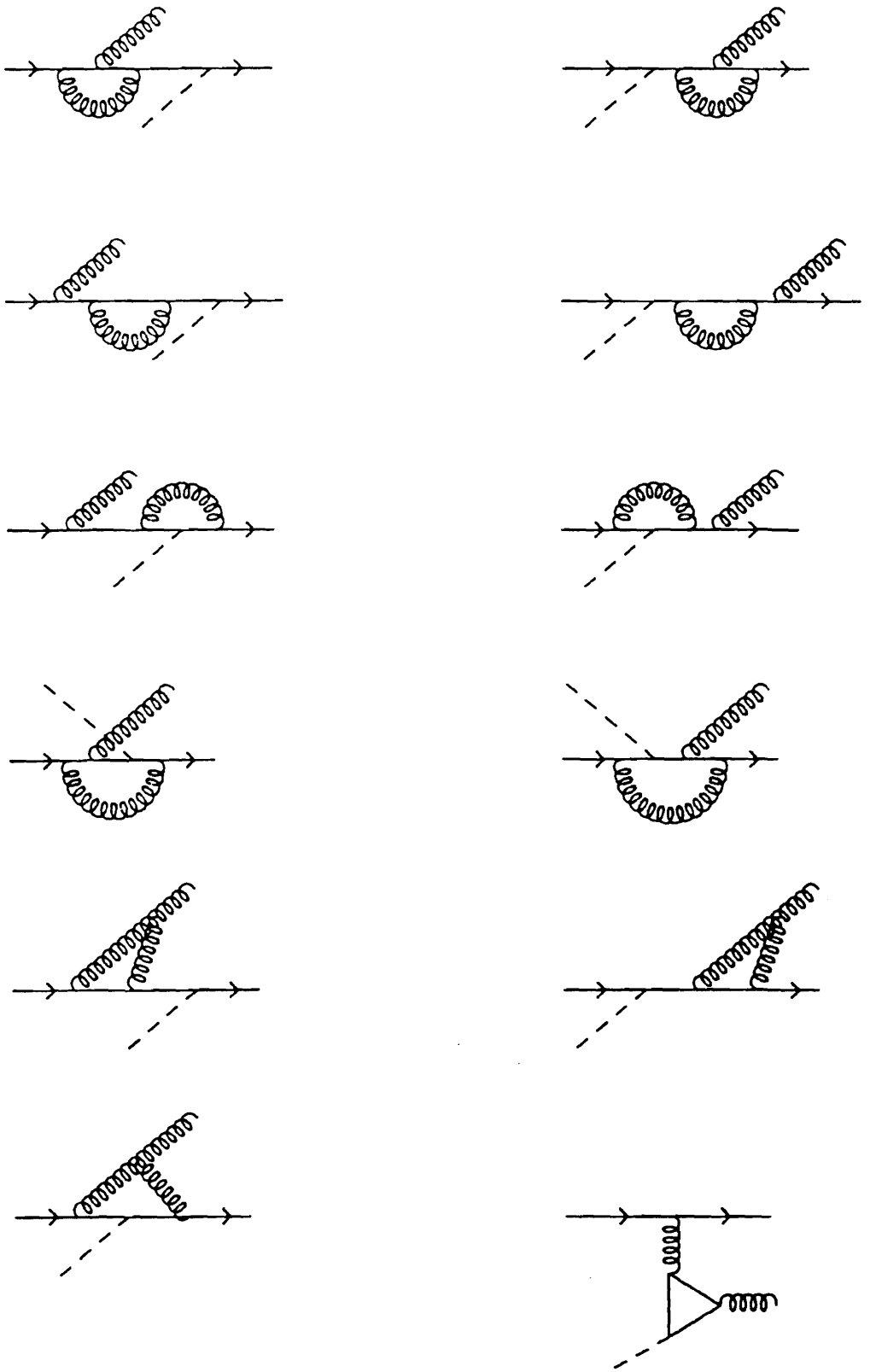

Fig. 6

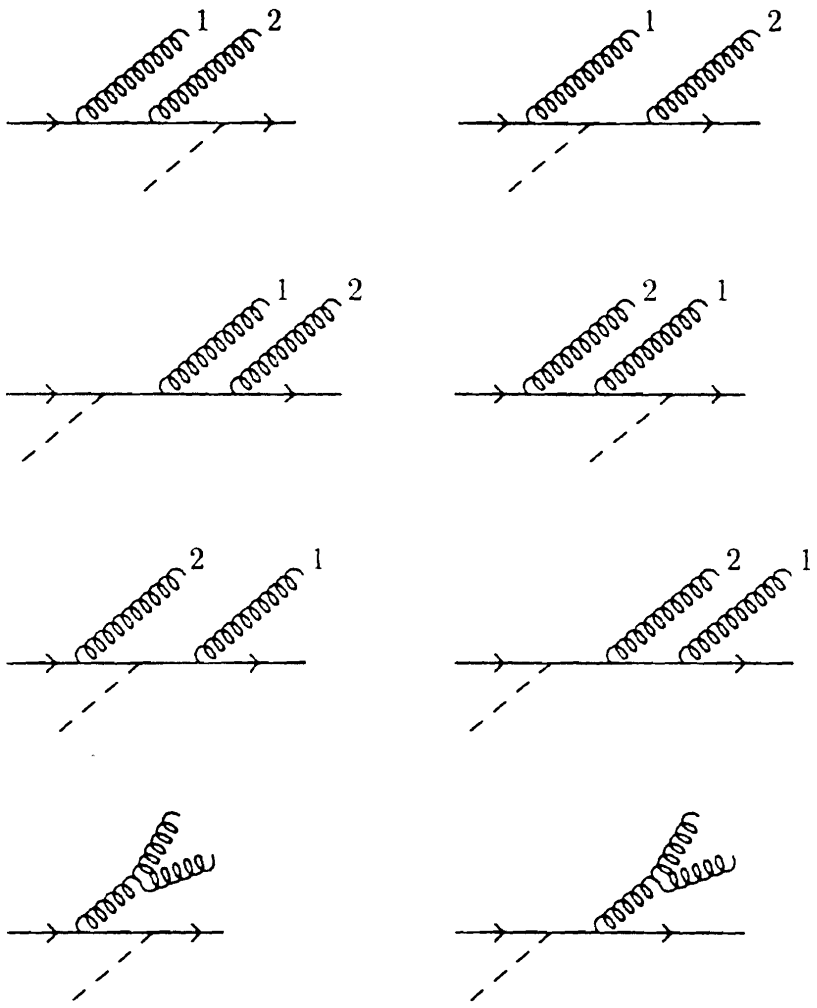

Fig. 7

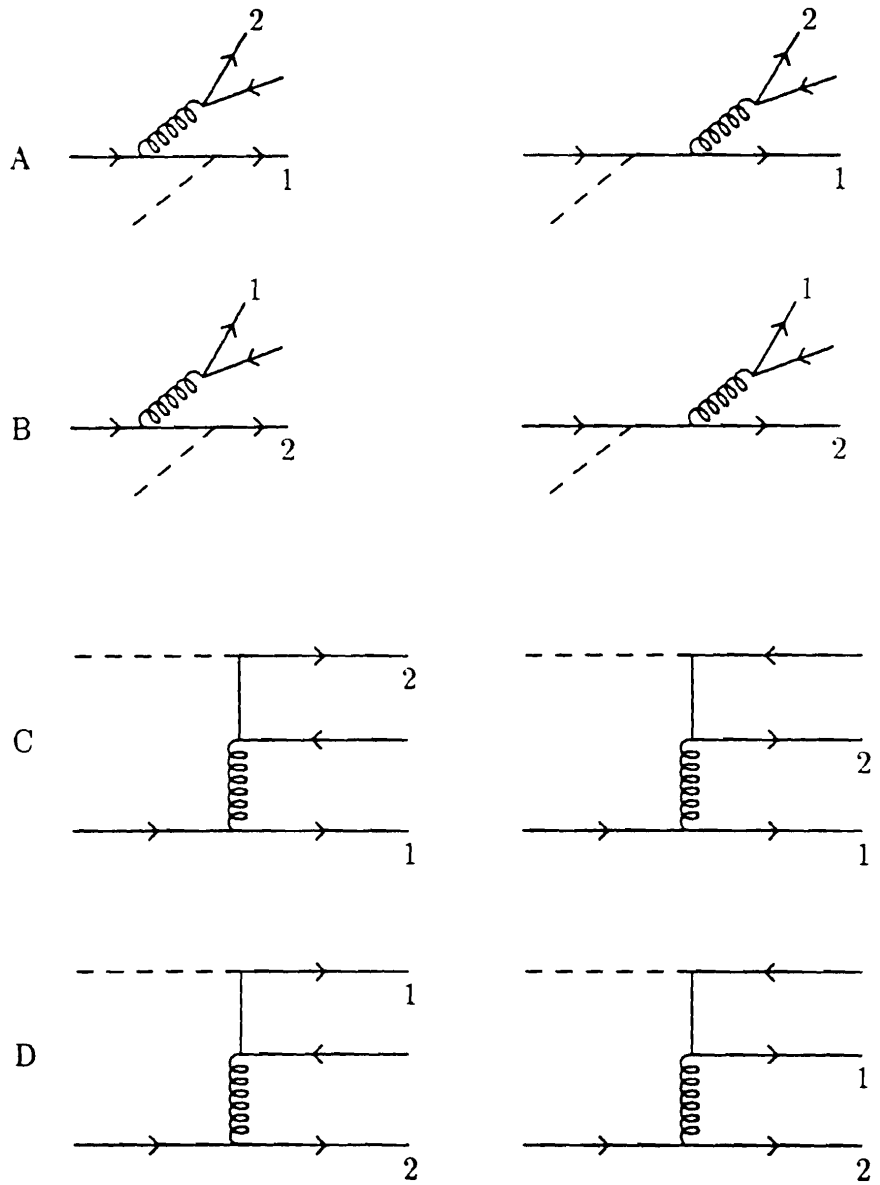

Fig. 8

Fig. 9

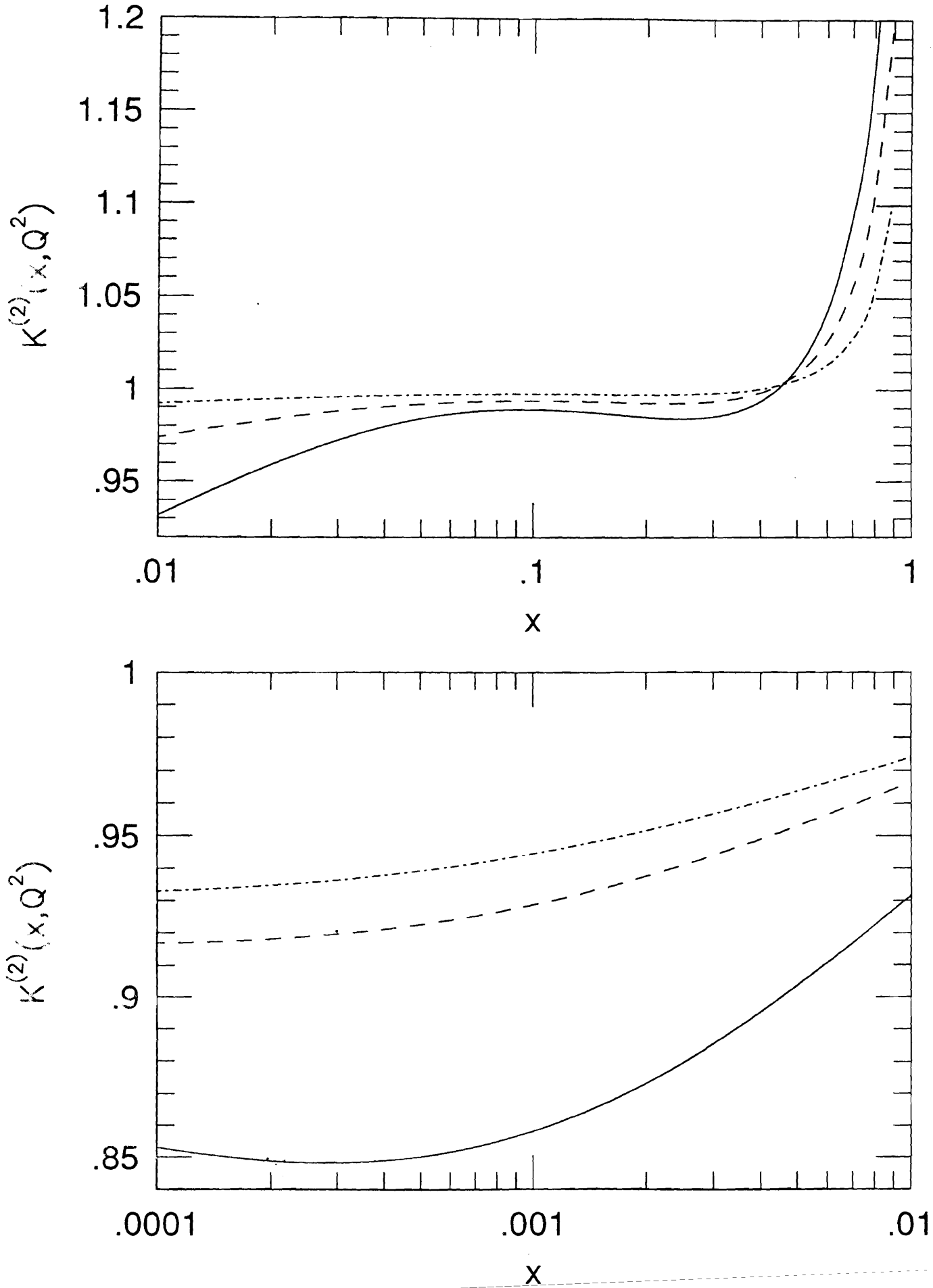

Fig. 10

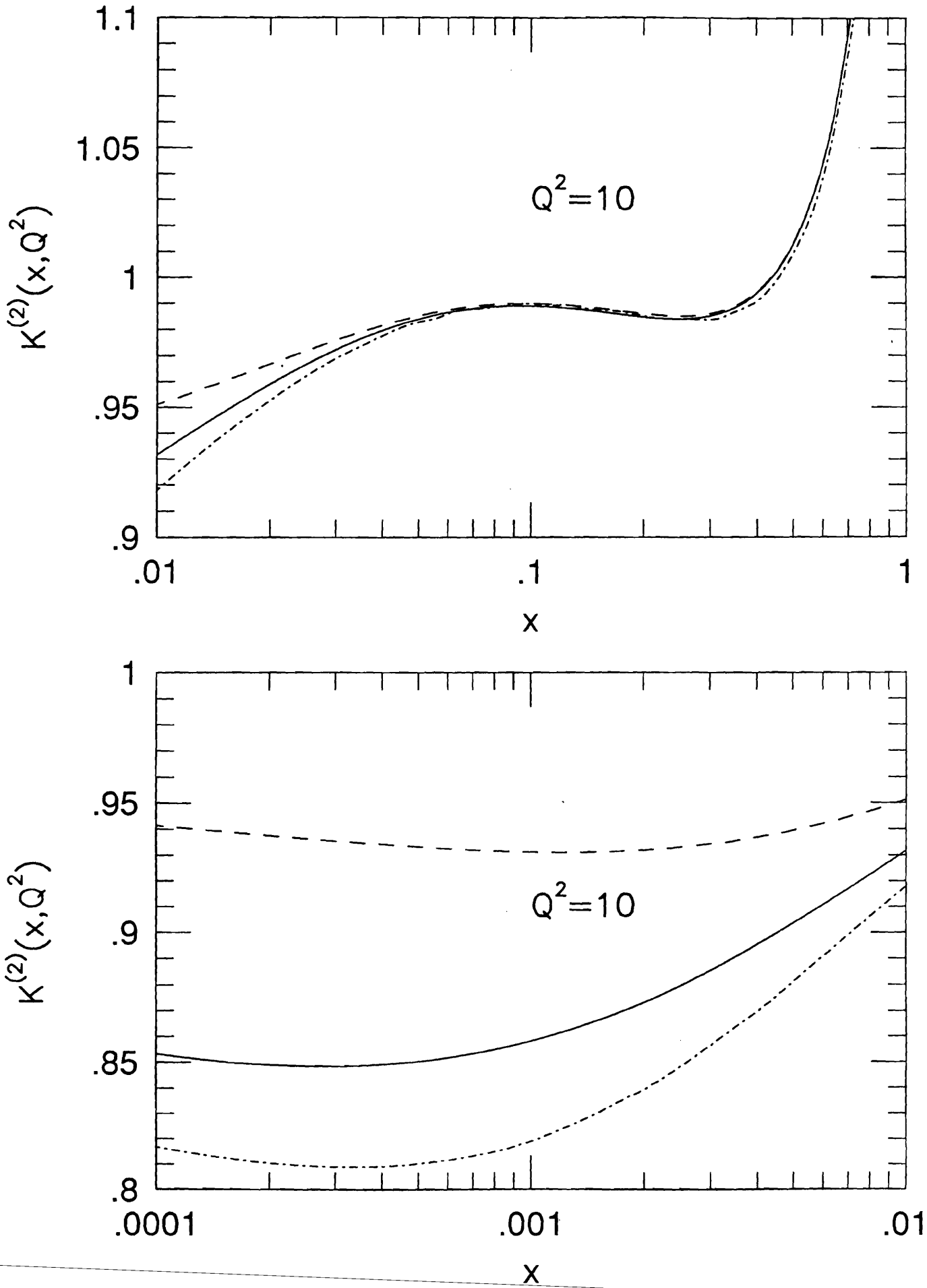

Fig. 11

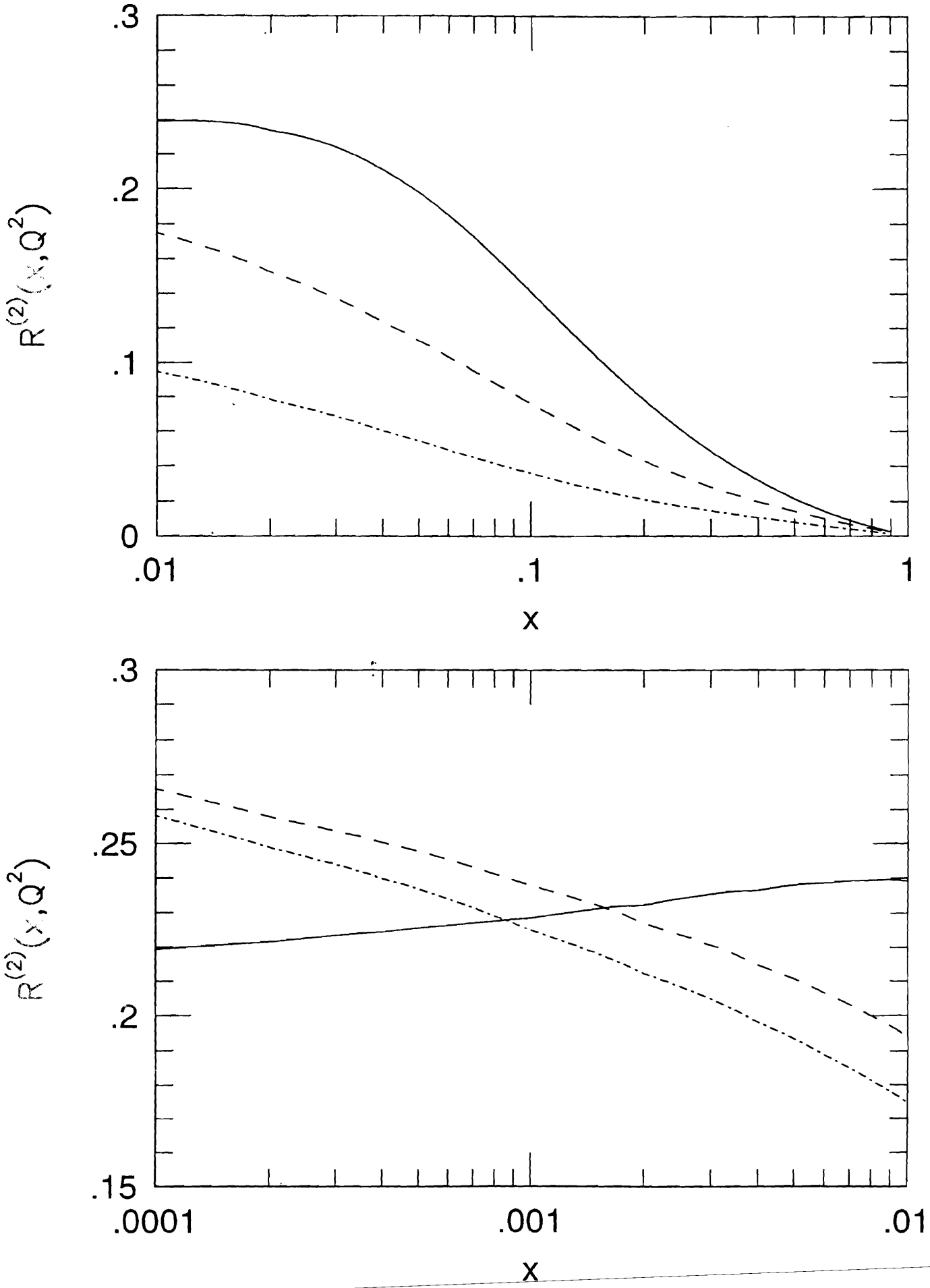

Fig. 12

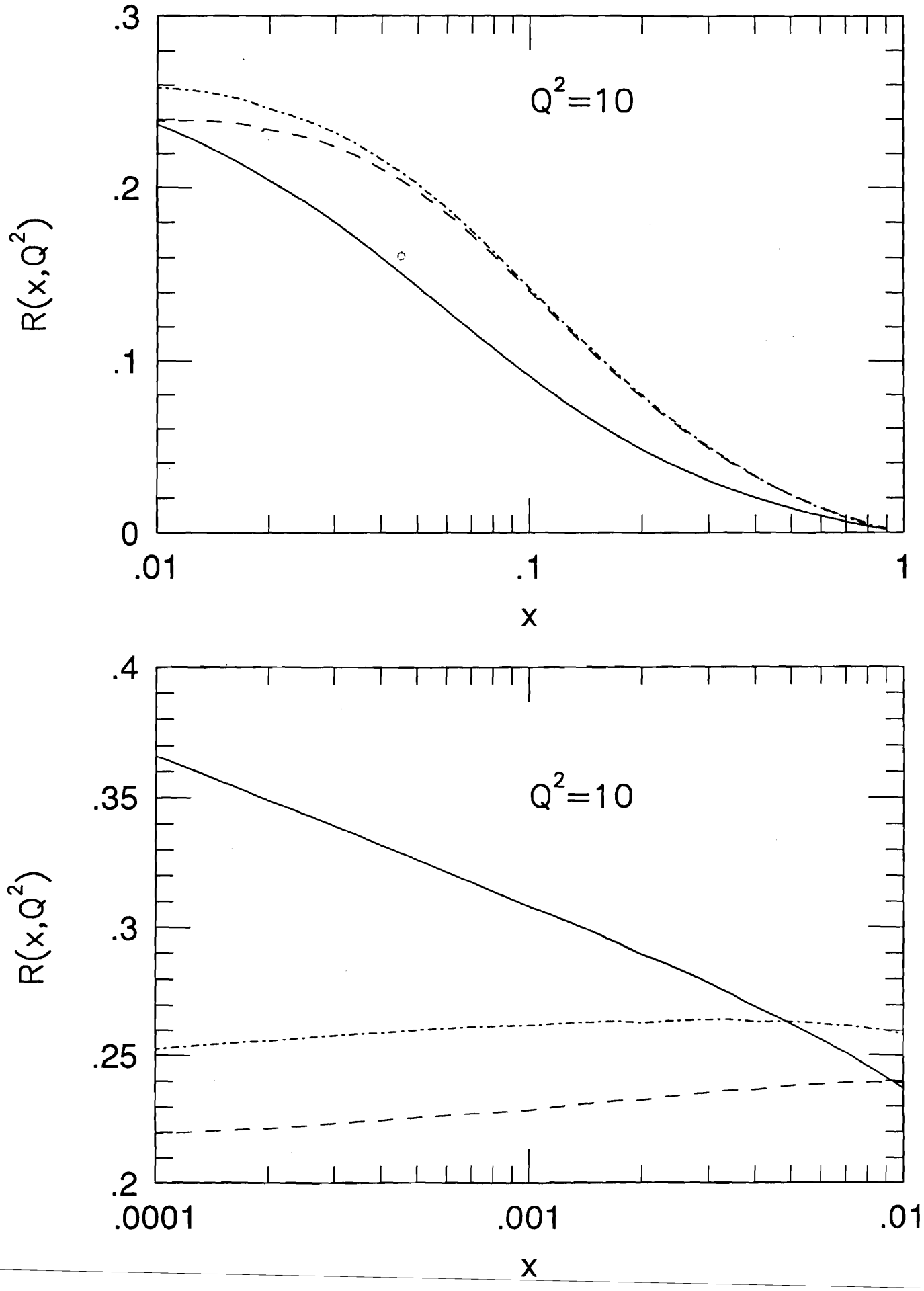

Fig. 13

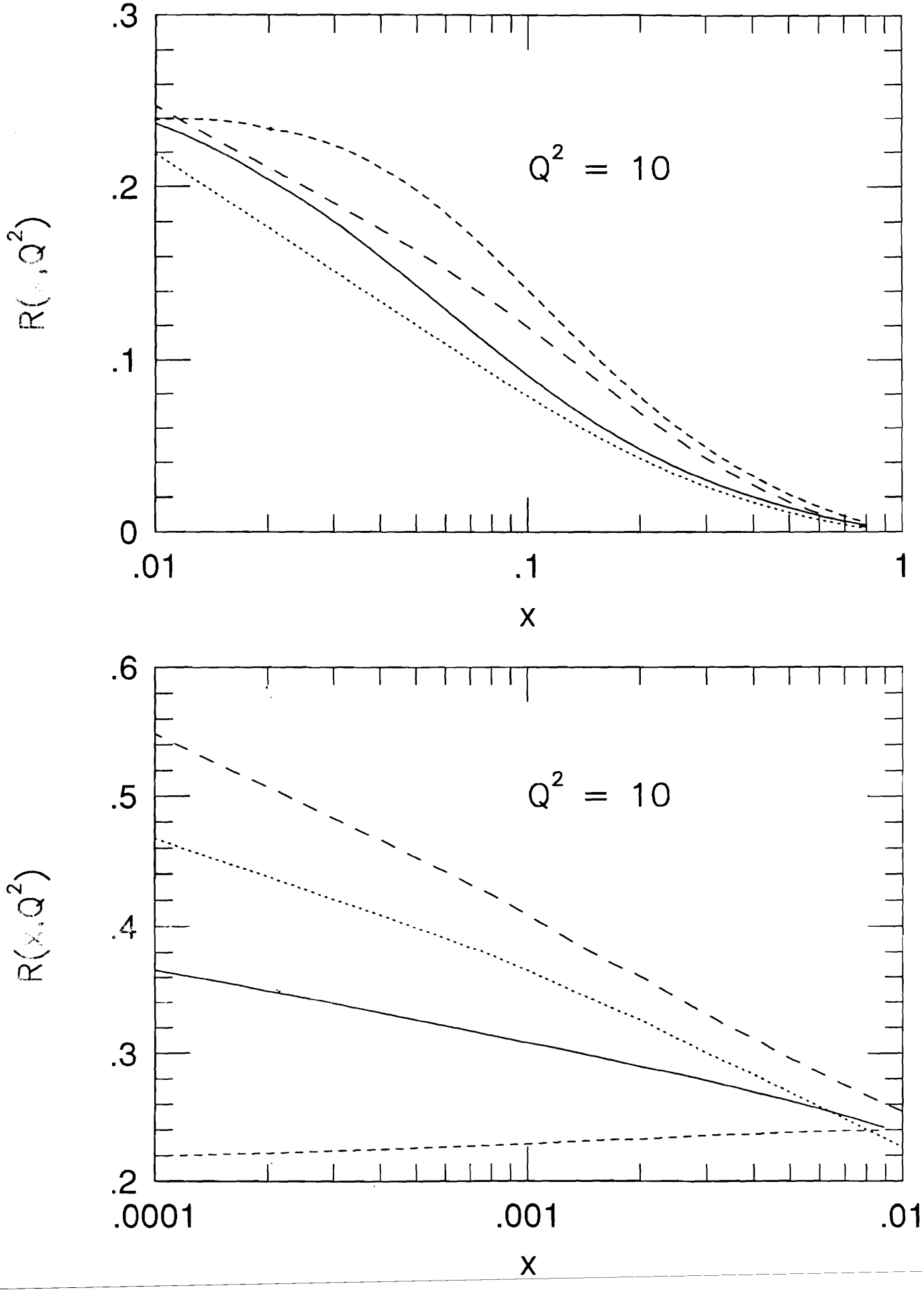

Fig. 14

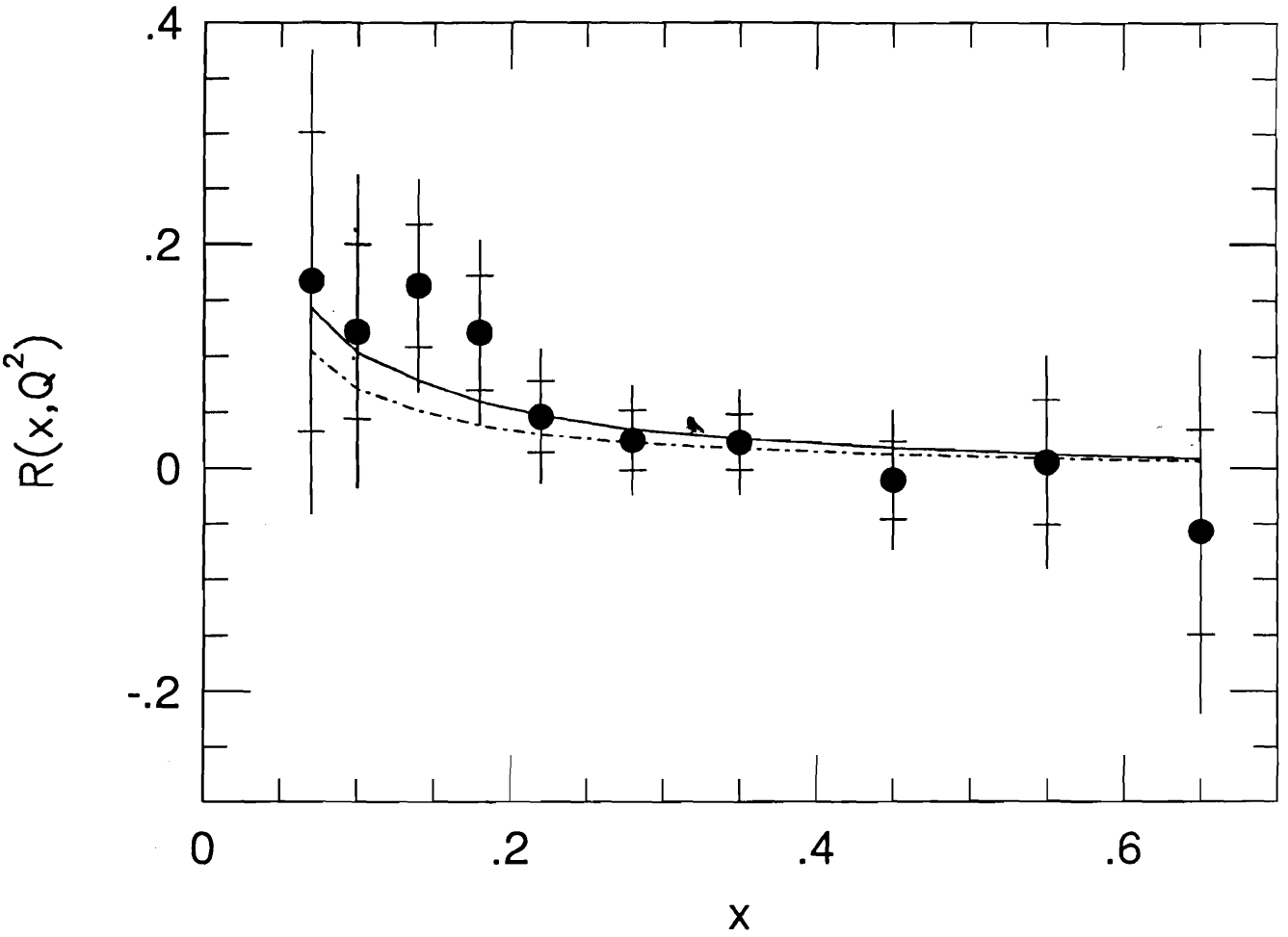

Fig. 15

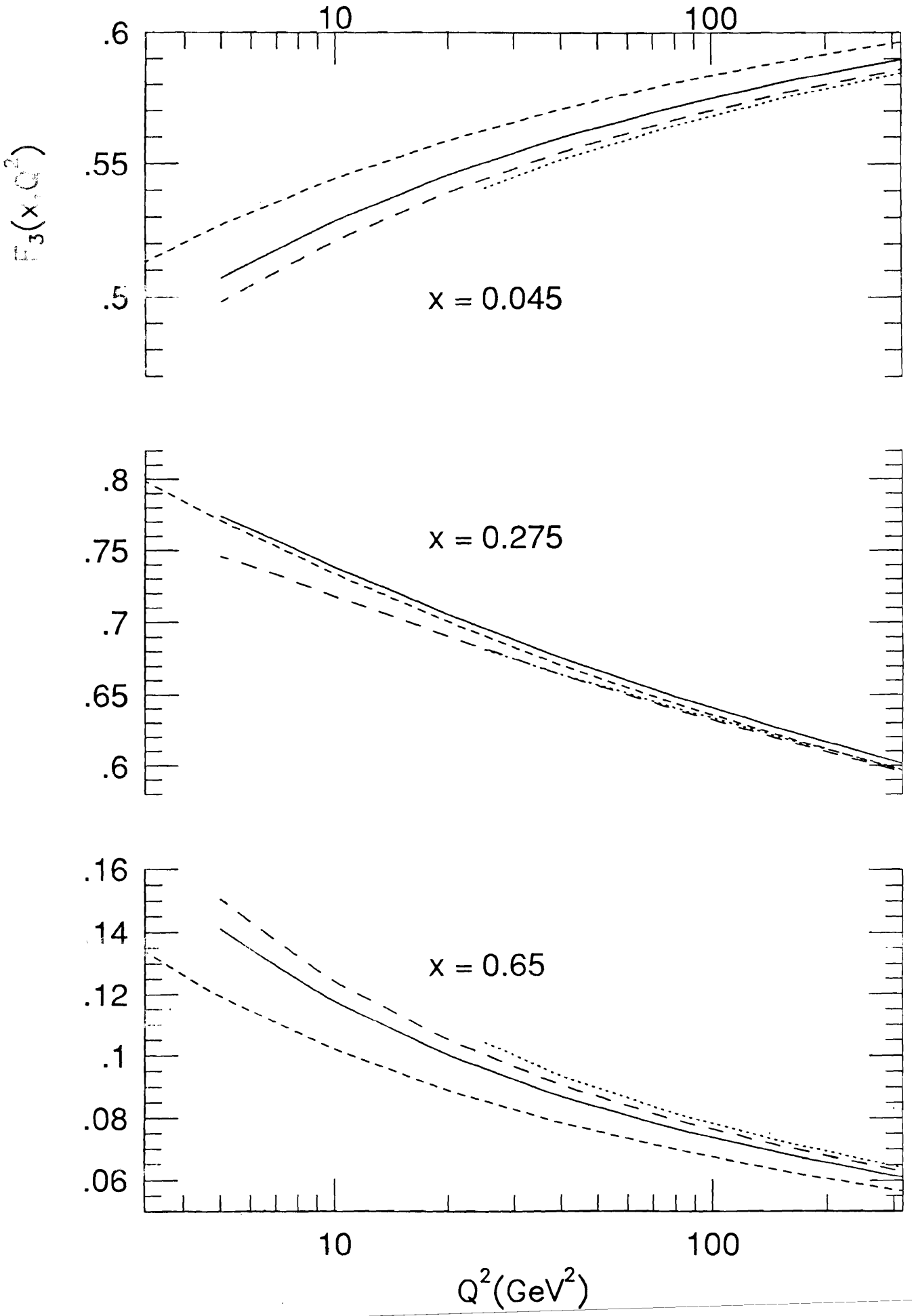
10
100
.6
.55
.5
$F_3(x,Q^2)$
x = 0.045
.8
.75
.7
.65
.6
x = 0.275
.16
.14
.12
.1
.08
.06
x = 0.65
10
100
$Q^2(GeV^2)$

Fig. 16

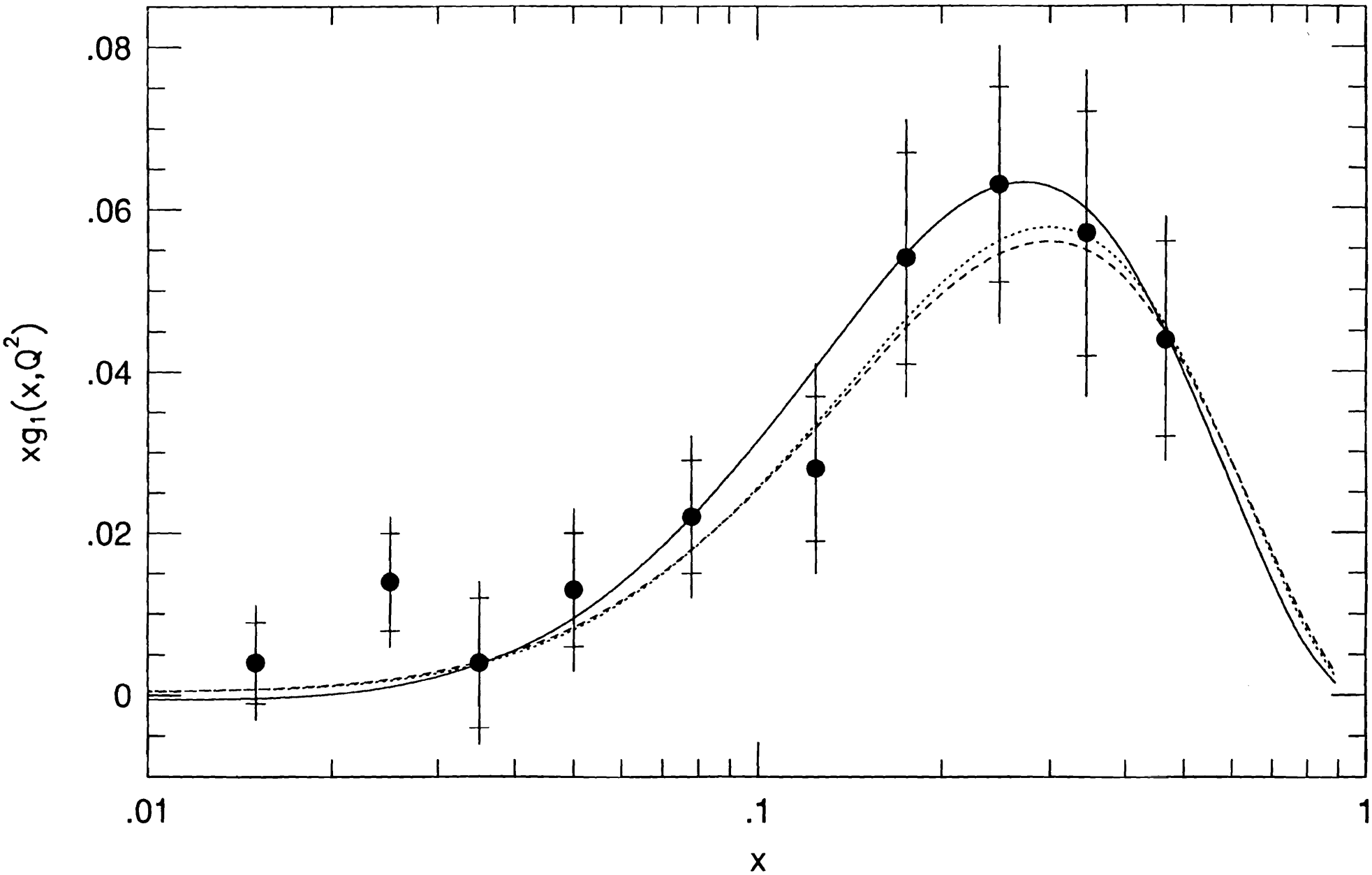

Fig. 17

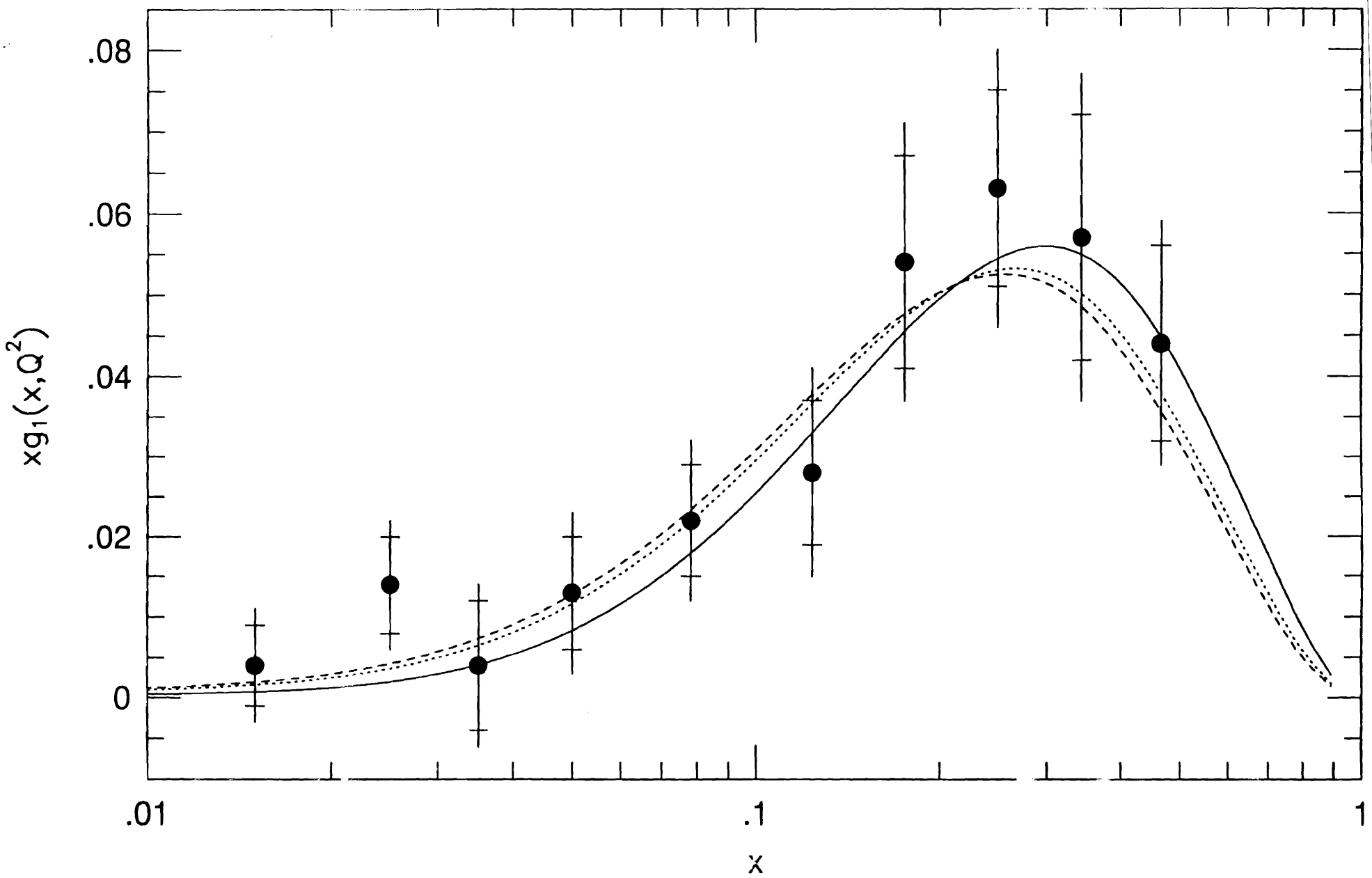

Fig. 18

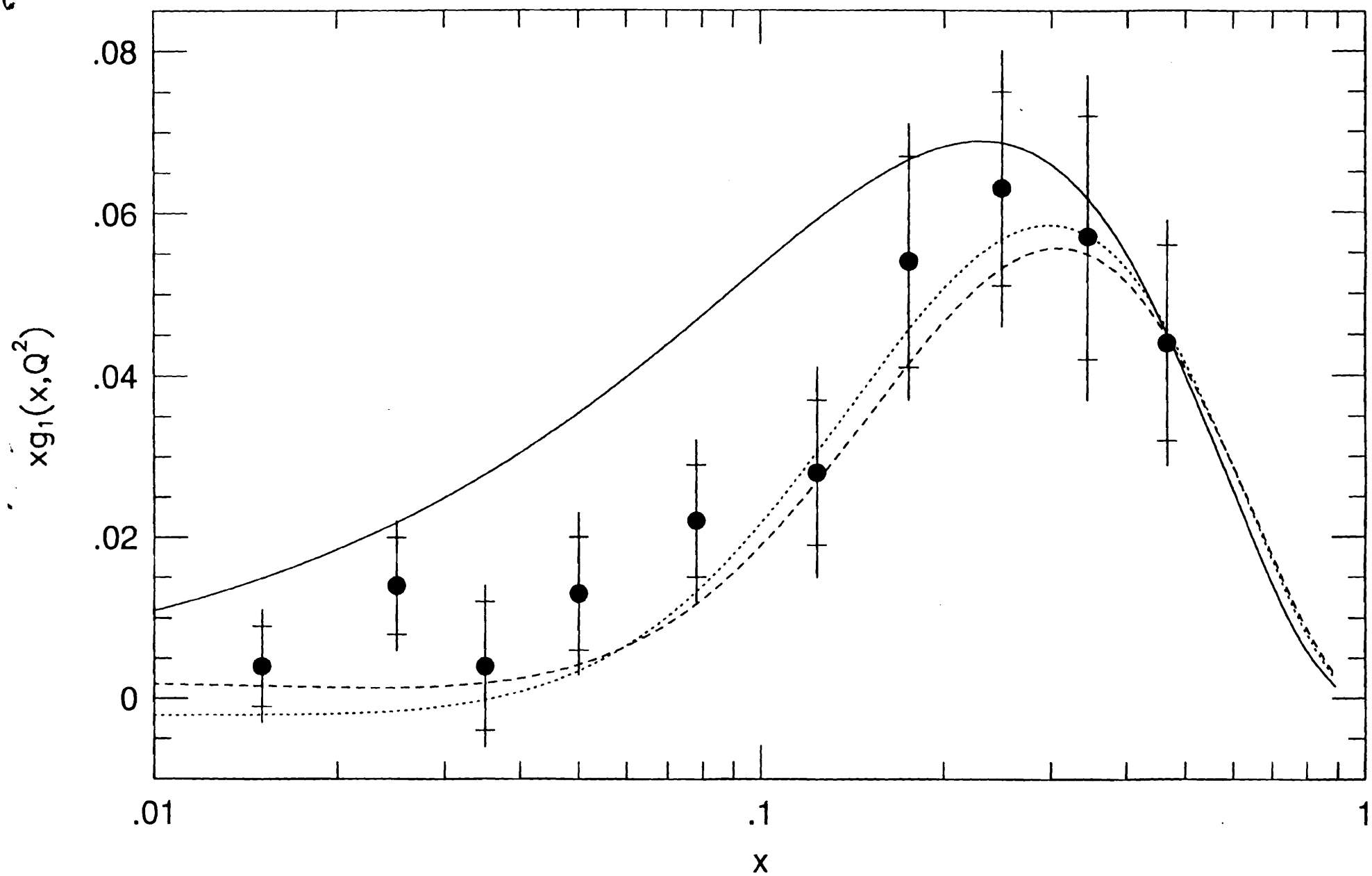
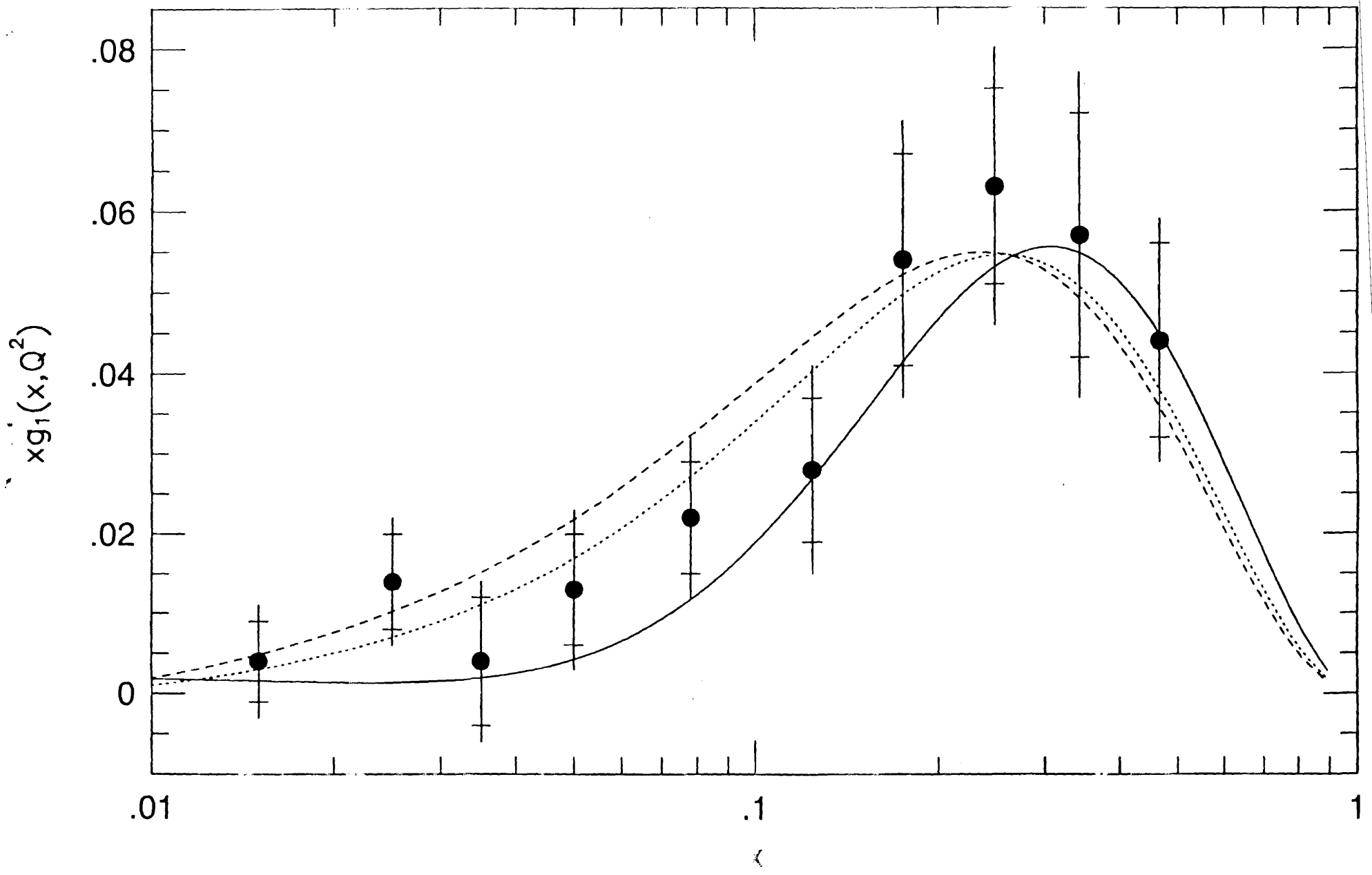
Fig. 19